Tissue recombination

Mouse UGM was prepared from 16-day embryonic mouse fetuses (plug date denoted as day 0) of pregnant WT or TN-C KO mice as previously described (Ishii et al., 2005). Briefly, urogenital sinuses were dissected from the fetuses and separated into epithelial and mesenchymal components by tryptic digestion and mechanical separation. Prostatic organoids of WT DLP or adult WT bladder urothelial cells were recombined with WT or TN-C KO UGM in neutralized type I rat tail collagen gels, and then tissue recombinants were grafted beneath the renal capsule of 8-week-old adult homozygous athymic CD-1 male nude mice (CLEA Japan, Inc., Tokyo, Japan).

Histopathology and immunohistochemistry

Serial sections (3 μm thick) were cut on a Leica RM2125 rotary microtome (Leica Microsystems, Wetzlar, Germany) and mounted on glass slides. Sections were deparaffinized in Histoclear (National Diagnostic, Atlanta, GA, USA) and hydrated in graded alcoholic solutions and running tap water. For histopathology, standard H&E and Masson's trichrome staining were carried out. Next, immunohistochemical staining was performed with a Vectastain ABC *Elite* kit (Vector laboratories Inc., Burlingame, CA, USA) following our protocol. After deparaffinization and hydration, endogenous peroxidase activity was blocked with 0.3% hydrogen peroxide in methanol for 20 min. After extensive washing in tap water, antigen retrieval was performed using 10 mM sodium citrate buffer of pH 6.0 for AR, Ki-67, and cleaved caspase-3. Antigen Unmasking Solution (Vector laboratories Inc., Burlingame, CA, USA) and 1.3 mg/mL pepsin solution were used for E-cadherin and uroplakin, and TN-C, respectively. For αSMA and γ-actin, antigen retrieval was not performed. Following a period of cooling and then rinsing in phosphate-buffered saline (PBS), the sections were incubated in blocking solution for at least 30 min at room temperature. The sections were then incubated with primary antibodies at 4 °C overnight. After incubation with primary antibodies, sections were incubated with appropriate biotinylated secondary anti-

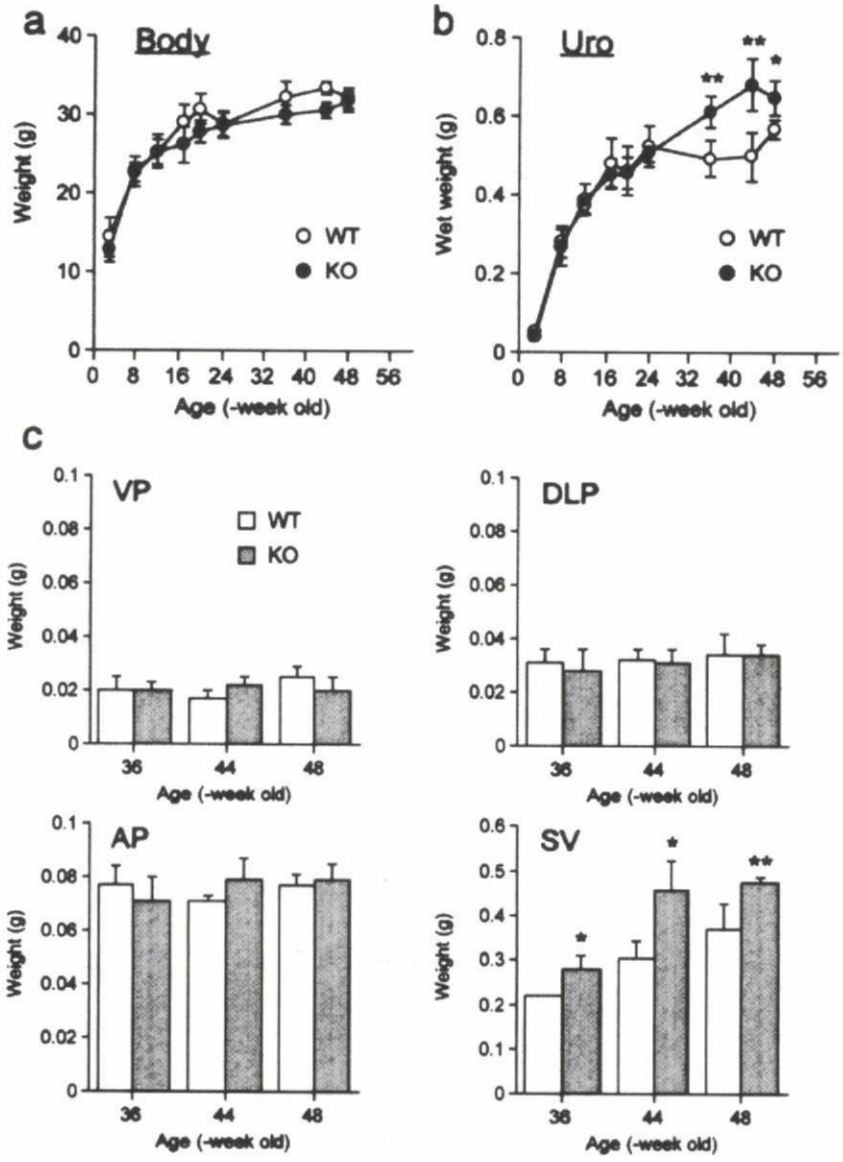

Fig. 2. No significant difference in prostatic weight of TN-C KO mouse. Body weight (a) and wet weight of mouse urogenital tract (b) from WT (○) and TN-C KO (●) were weighted at various ages. (c) Wet weights of microdissected lobes from WT (□) and TN-C KO (■) are indicated for various ages. VP: ventral prostate, DLP: dorsolateral prostate, AP: anterior prostate, SV: seminal vesicle. Values represent the means ± S.D. * $p<0.05$, ** $p<0.01$ versus WT.

mouse, anti-rabbit, or anti-rat immunoglobulin included in the ABC *Elite* kit for 30 min at room temperature. The antigen–antibody reaction was visualized using 3,3′-diaminobenzidine tetrahydrochloride (DAB) as a substrate. Sections were counterstained with hematoxylin and examined by light microscopy. Anti-AR, E-cadherin, Ki-67, αSMA, γ-actin, cleaved caspase-3, uroplakin, and TN-C were used at dilutions of 1:300, 1:3000, 1:100, 1:10,000, 1:1000, 1:400, 1:50, and 1:1000, respectively. The number of binucleated cells was determined by E-cadherin immunostaining in ten separate microscopic fields (×400) from each tissue specimen.

Statistical analysis

The results were expressed as the means±S.D. Differences between the two groups were determined using Student's *t*-test. Values of $p<0.05$ were considered statistically significant.

Table 1
Comparisons of cell proliferation and apoptotic incidence between WT and TN-C KO mice

	WT		TN-C KO	
	Epi	Stroma	Epi	Stroma
Cell proliferation (%)				
AP	2.4±1.7	1.1±2.5	0.9±0.4	4.1±5.0
DLP	0.3±0.7	1.1±2.5	0.3±0.4	0±0
VP	0.9±1.3	0±0	1.6±1.6	0±0
Apoptosis (%)				
AP	0.5±1.1	0±0	0±0	0±0
DLP	0±0	0±0	0±0	0±0
VP	0±0	0±0	0.4±0.9	0±0

Cell proliferation and apoptotic incidence in 17-week-old mice were analyzed by Ki-67 immunostaining and cleaved caspase-3 immunostaining, respectively. Values represent the means±S.D. from at least 5 ducts.

Results

Expression of TN-C in prostate of WT mice

We separated all mouse prostates from 17-week-old into three lobes each: anterior prostate (AP), dorsolateral prostate (DLP), and ventral prostate (VP), as previously reported (Sugimura et al., 1986). In WT mouse, ducts of all prostatic lobes were lined by luminal secretory epithelial cells with basally located nuclei (Fig. 1). Immunostaining for αSMA and smooth muscle γ-actin, a late marker for smooth muscle differentiation (Qian et al., 1996), showed that prostatic ducts were generally surrounded with thin stromal smooth muscle layers (Figs. 1b, c, e, f, h, i). TN-C was localized beneath the basement membrane surrounding prostatic ducts as previously reported in rat prostate (Vollmer et al., 1994a) (Figs. 1a, d, g).

Morphological phenotype of TN-C KO mouse prostate

There was no significant difference in body weights between WT and TN-C KO mice (Fig. 2a). Wet weights of urogenital tract including all prostatic lobes and the SV in TN-C KO mouse were significantly heavier than those in WT mouse between 36 weeks and 48 weeks of age ($p<0.05$) (Fig. 2b). The SV weights in TN-C KO mouse were significantly heavier than those in WT mouse ($p<0.05$) (Fig. 2c),

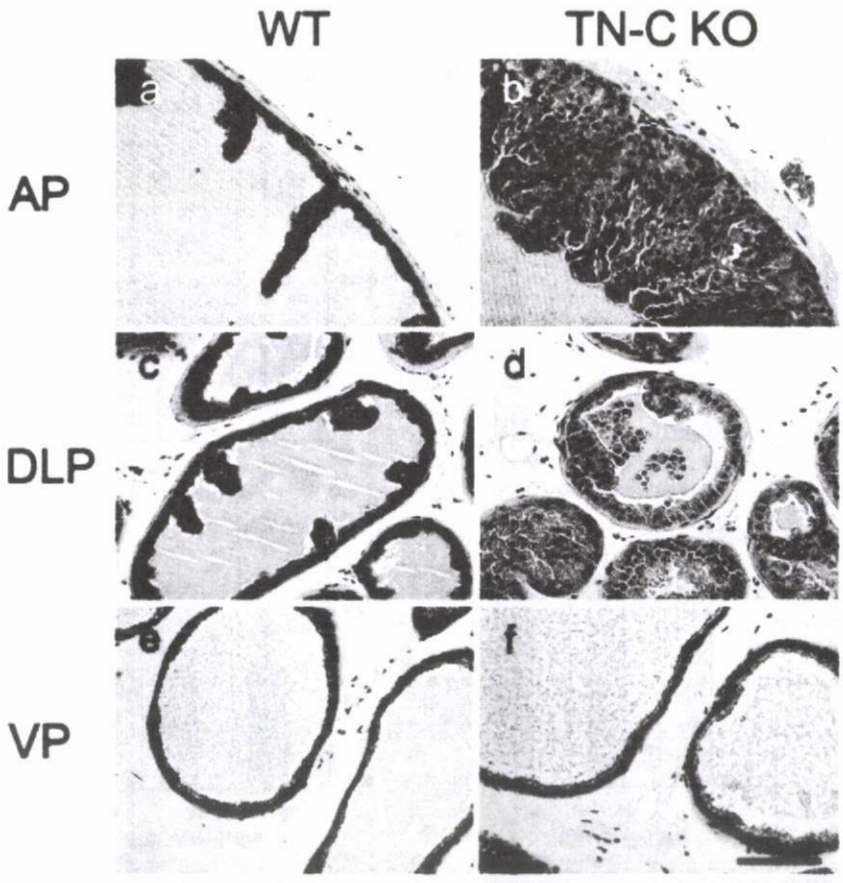

Fig. 3. Morphological phenotype of TN-C KO mouse prostate. All sections from 17-week-old mice were H&E stained. The corresponding sections from AP, DLP, and VP are shown in panels a, c, and e for WT, and in panels b, d, f for TN-C KO. Scale bar=100 μm, magnification ×200.

although there were no significant differences among individual prostatic lobe weights between WT and TN-C KO mice.

In TN-C KO mouse, multilayered epithelial clusters protruded into the ductal lumens in the AP (Fig. 3b) and also in the DLP, but to a lesser extent (Fig. 3d). The multilayered epithelium appeared at 8 weeks, and was maintained thereafter to at least 48 weeks. Although the stroma in TN-C KO prostate tended to be thicker than that in WT prostate, there was no aggressive phenotype of stromal component such as hypercellular stroma or spindled stroma (Ishii et al., 2005). Accumulation of collagen was not observed by Masson's trichrome staining (data not shown). No significant increase of cell proliferation or decrease of apoptotic incidence in epithelial or stromal component was found by analyses of Ki-67 labeling index or caspase-3 labeling index when examined at 17 weeks, respectively (Table 1). The TN-C KO VP appeared morphologically normal as compared with the WT VP (Figs. 3e, f). In the TN-C KO SV, there was no apparent morphological difference such as epithelial hyperplasia or hypercellular stroma (data not shown).

Histological analysis in TN-C KO mouse prostate

Binucleated cells, having two nuclei in individual epithelial cells surrounding E-cadherin-positive membrane, were shown in glands of the TN-C KO AP and DLP (Figs. 4b, d). In WT mouse, however, binucleated cells were rarely observed (Figs. 4a, c). The number of binucleated cells in the TN-C KO DLP was significantly increased from 8 weeks to 48 weeks of age, accompanied with multilayered epithelial growth ($p<0.05$) (Fig. 4e).

The expression of AR was detected in nuclei of both epithelial and stromal cells of the WT AP and DLP (Figs. 5a, c). Interestingly, in TN-C KO mice, AR-positive epithelial cells were decreased in the AP lobe, and most epithelial cells in the DLP were AR-negative; stromal cells surrounding the ducts were AR-positive ($p<0.01$) (Figs. 5d, e). The percentage of AR-negative epithelial cells in the AP was quite low compared to that in the DLP in TN-C KO mice (Figs. 5b, e). No significant difference in AR expression was observed between WT and TN-C KO VP (Fig. 5e).

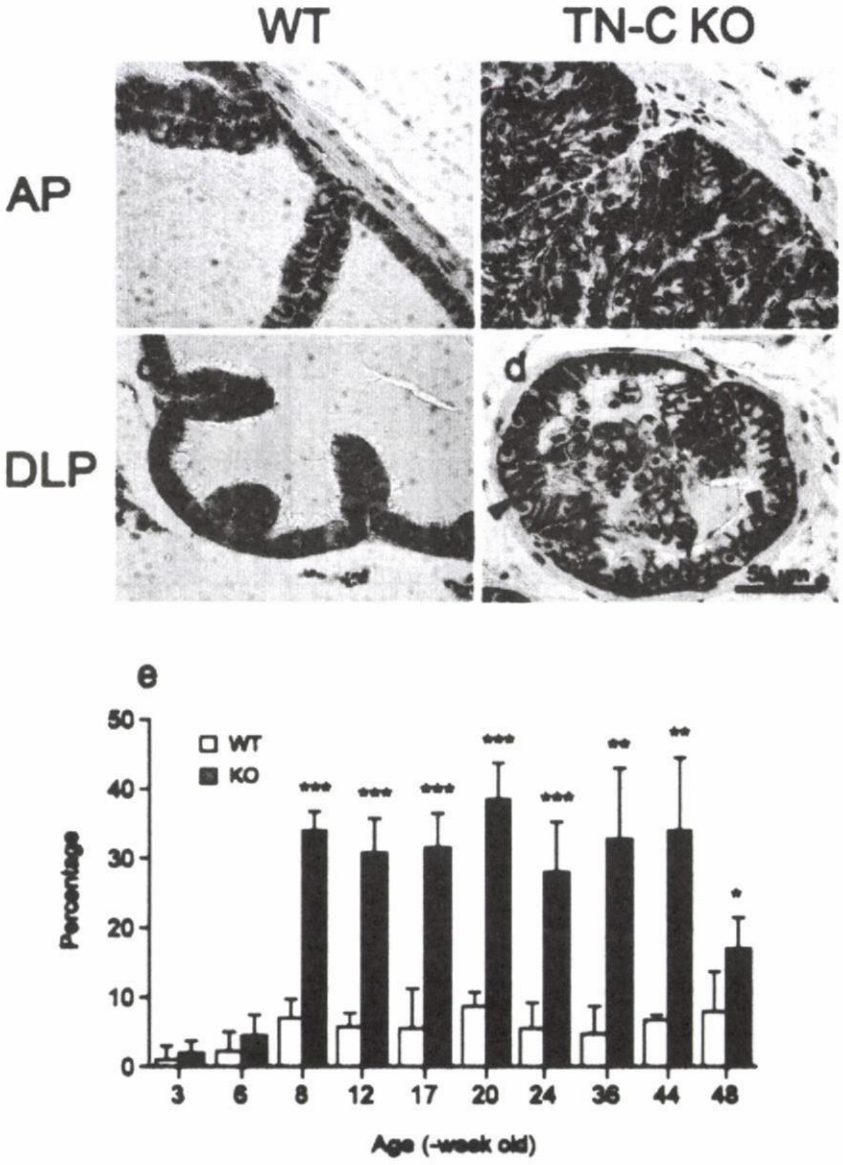

Fig. 4. Appearance of binucleated cells in TN-C KO mouse prostate. (a–d) The histopathology of WT and TN-C KO mouse prostate was examined with E-cadherin immunostaining. The corresponding sections from AP and DLP are shown in panels a and c for WT, and in b and d for TN-C KO. Arrowheads indicate the binucleated cells. Scale bar = 50 μm, magnification ×400. (e) The number of binucleated cells in each DLP duct of WT (□) and TN-C KO (■) was counted at various ages. Values represent the means ± S.D. from at least 5 ducts. * $p<0.05$, ** $p<0.01$, *** $p<0.001$ versus WT.

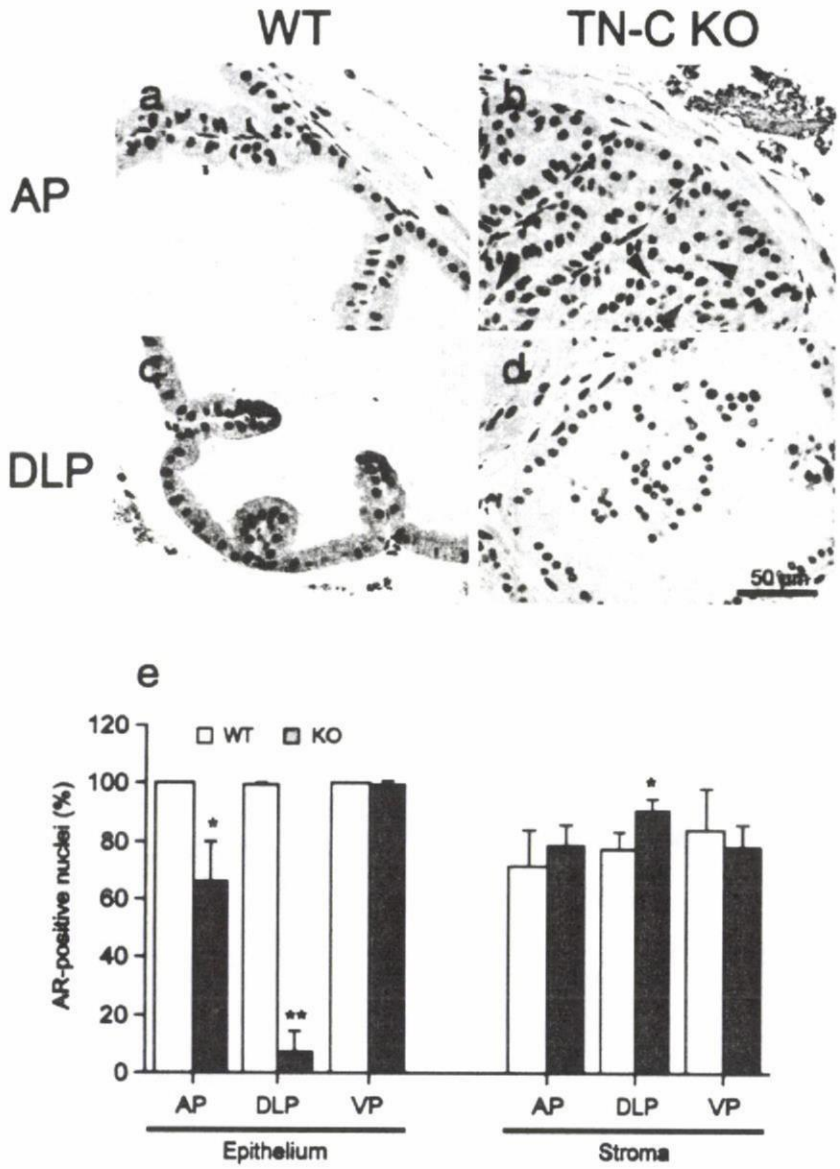

Fig. 5. Loss of AR expression in the epithelium of TN-C KO mouse prostate. (a–d) AR expression was assessed by immunostaining in WT and TN-C KO mouse prostate. The corresponding sections from AP and DLP are shown in panels a and c for WT, and in panels b and d for TN-C KO. Arrowheads indicate the AR-negative nuclei. Scale bar = 50 μm, magnification ×400. (e) The number of AR-positive nuclei in each prostatic duct of WT (□) and TN-C KO (■) was counted at 17 weeks of age, and then the percentage of AR-positive cells was calculated. Values represent the means ± S.D. for at least 5 ducts. * $p<0.01$, ** $p<0.0001$ versus WT.

Tissue recombination with fetal TN-C KO UGM

To examine whether TN-C deficiency in prostatic stroma affected epithelial growth and differentiation, we performed tissue recombination between adult WT DLP epithelium and UGM of WT or TN-C KO mice, and then grafted recombinants beneath the renal capsule (Figs. 6a, b). Recombinants were examined at 4 weeks postgrafting. Control recombinants with WT UGM showed normal-appearing prostatic glandular epithelium exhibiting normal secretory differentiation (Fig. 6c) and with a thin layer of stroma similar to that of intact WT mouse prostate, as described previously (Ishii et al., 2005).

In contrast, tissue recombinants prepared with TN-C KO UGM and adult WT prostatic epithelium showed morphological phenotypes including multilayered epithelial clusters, binucleated cells, and AR-negative nuclei, similar to those in TN-C KO mouse prostate (Figs. 6d, f, h). Histological analysis such as αSMA immunostaining and Masson's trichrome staining showed no significant difference in the stromal component adjacent to prostatic epithelia between WT and TN-C KO recombinants (data not shown). Thus, these findings indicate that TN-C-null mesenchymal components can induce the morphological changes in WT prostate glands in tissue recombinants similar to that seen in TN-C KO mice.

To investigate whether TN-C-null mesenchymal components can induce urothelial transdifferentiation to prostatic epithelia, we next performed tissue recombination between adult WT bladder urothelial cells and UGM of WT or TN-C KO mice (Fig. 7). Control recombinants with WT UGM showed induction of normal-appearing prostatic glandular structure from adult bladder urothelial cells, as expected (Figs. 7a, c, e, g). In contrast, tissue recombinants with TN-C KO UGM showed morphological differences with no prostatic secretion in the lumen (Figs. 7b, d). Detailed histological analyses showed that some AR-positive epithelial cells appeared but uroplakin-positive bladder urothelial cells still remained in the resultants with TN-C KO UGM+

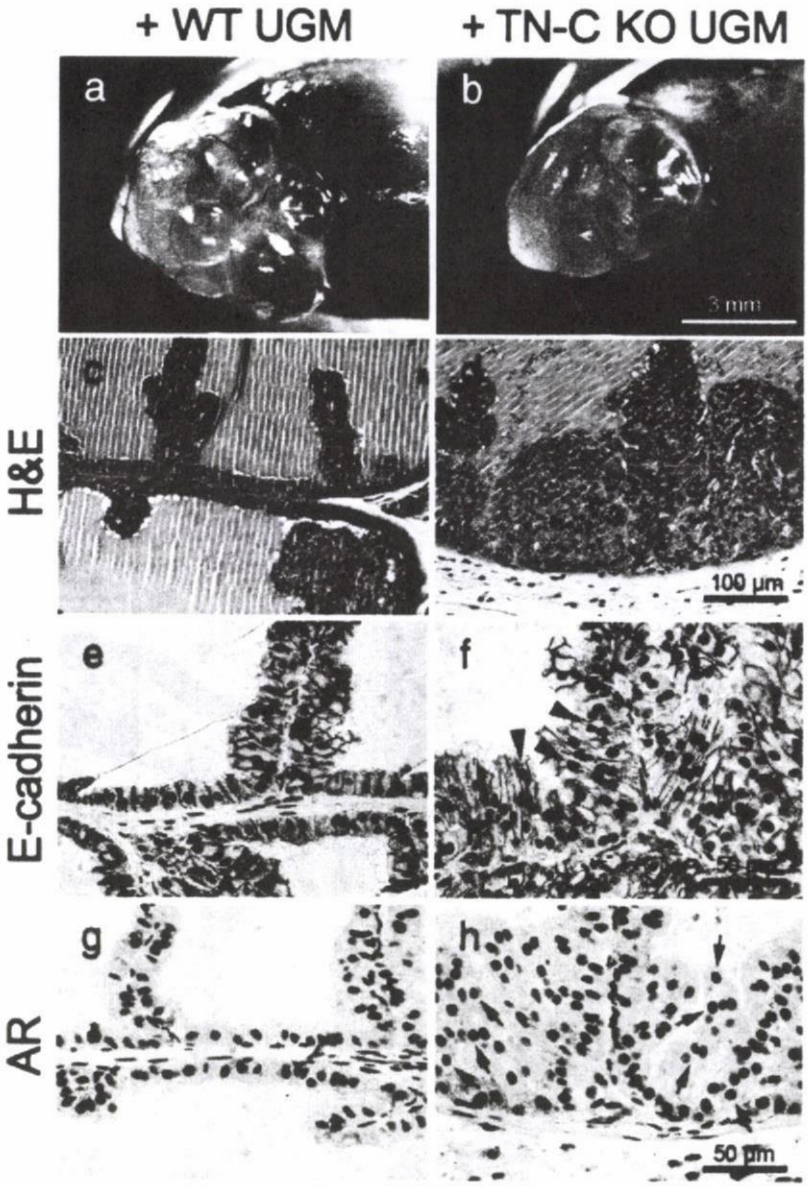

Fig. 6. Tissue recombinants composed of adult WT DLP epithelium and fetal TN-C KO UGM. (a–d) Gross appearances of WT and TN-C KO recombinants are shown in panels a and b, respectively. Vascularized cystic mass is observed on the host kidney (K). The histopathology was examined with H&E staining shown in c for WT and d for TN-C KO recombinants. Scale bar = 100 μm, magnification ×200. (e–h) Detailed histopathological characteristics were examined with expression of E-cadherin (e and f) and AR (g and h). The corresponding sections from tissue recombinants are shown in panels e and g for WT, and in panels f and h for TN-C KO. Arrowheads and arrows indicate the binucleated cells and the AR-negative nuclei, respectively. Scale bar = 50 μm, magnification ×400.

bladder epithelium tissue recombinants (Figs. 7f, h). These results indicate that stromal TN-C participates in urothelial transdifferentiation to prostatic epithelia.

Discussion

TN-C is often induced in response to mesenchymal–epithelial interactions that initiate organogenesis and morphogenesis (Chiquet-Ehrismann et al., 1986). Mesenchymal–epithelial interactions play crucial roles in morphogenesis and cytodifferentiation in the development of the prostate (Cunha, 1976). However, it has been proposed that TN-C might not be involved in the early morphogenesis of the prostatic buds, because little TN-C was detected in the mesenchyme around developing prostatic buds (Takeda et al., 1988). In adult prostate, stroma composed of smooth muscle cells also interact with glandular epithelia. These stromal–epithelial interactions maintain functional differentiation and growth-quiescence of glandular epithelia (Hayward et al., 1997). Deregulation of the stromal–epithelial interactions is considered to be responsible for the initiation and/or promotion of prostatic diseases such as benign prostatic hyperplasia (BPH) and prostate carcinoma (PCa) (Olumi et al., 1999; Bhowmick et al., 2004). Since increased TN-C expression has been observed in these lesions (Ibrahim et al., 1993; Xue et al., 1998), many recent studies have focused on the role of TN-C in prostate cancer progression (Tomas et al., 2006; Tuxhorn et al., 2002).

To investigate TN-C functions in organogenesis and morphogenesis, TN-C KO mice were independently generated by two different groups (Saga et al., 1992; Forsberg et al., 1996). Both groups have reported the same findings, that TN-C deficient mice undergo normal in development and have a normal life span and fertility in mice. TN-C

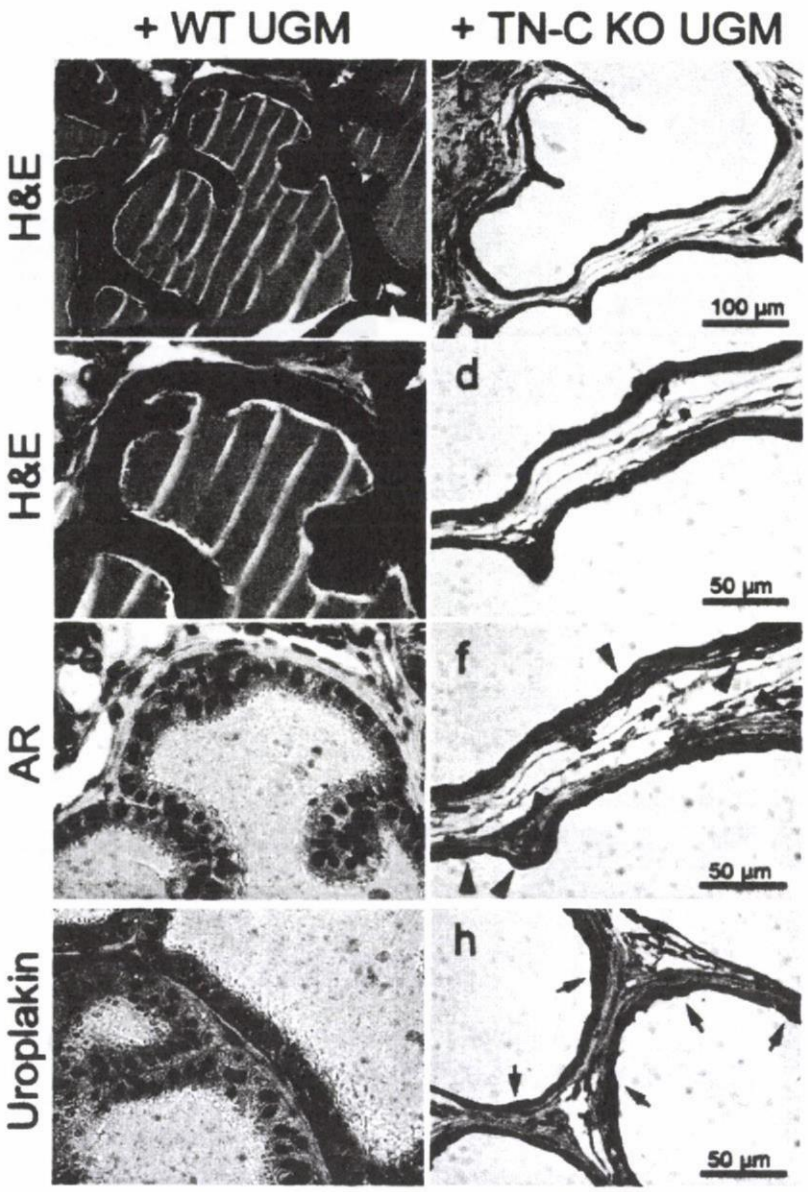

Fig. 7. Tissue recombinants composed of adult WT bladder urothelial cells and fetal TN-C KO UGM. (a–d) The histopathology was examined with H&E staining shown in panels a and c for WT or panels b and d for TN-C KO recombinants. Scale bar = 100 μm, magnification ×200. Scale bar = 50 μm, magnification ×400. (e–h) Detailed histopathological characteristics were examined with expression of AR (e and f) and uroplakin (g and h). The corresponding sections from tissue recombinants are shown in panels e and g for WT, and in panels f and h for TN-C KO. Arrowheads and arrows indicate the AR-positive cells and the uroplakin-positive cells, respectively. Scale bar = 50 μm, magnification ×400.

null mice did not show any morphological phenotype in the principal organs such as heart, lung, thymus, and cerebellum (Saga et al., 1992; Imanaka-Yoshida et al., 2003). However, more detailed investigations have shown differences in specific cell behavior and response to external stimuli in adult (Ohta et al., 1998; Fukamauchi et al., 1997; Tamaoki et al., 2005). Decreased bronchial branching and enlarged airspaces have been found in lung development of TN-C KO mice (Roth-Kleiner et al., 2004). Recently we have also reported that TN-C deficiency attenuates allergic inflammation in bronchial asthma and liver fibrosis in chronic hepatitis (Nakahara et al., 2006; El-Karef et al., 2007).

The present study demonstrated that the prostate in TN-C KO mice developed and grew almost normally. However, with careful microscopical analysis, we observed multilayered ductal epithelia and binucleated cells in AP and DLP lobes of TN-C KO mice. Tissue recombinants using fetal TN-C KO UGM and adult prostatic epithelia elicited similar morphological changes in prostatic epithelia, indicating that deficiency of stromal TN-C causes the glandular phenotypes. In addition, it was found that a certain population of these abnormal glandular epithelia failed to express AR proteins both *in vivo* and in TN-C KO UGM+ WT prostatic epithelium tissue recombinants. Therefore, it is suggested that stromal TN-C plays an important role in maintaining adult prostatic ductal morphology. The SV weights in TN-C KO mouse were significantly heavier than those in WT mouse, while the glandular change was not observed. Epithelial clusters of AP and DLP protruding into ductal lumen may cause obstruction, followed by retention of seminal fluid in the SV.

In regard to the role of TN-C as a stromal morphogenic signal that drives epithelial cell differentiation, we further investigated the effects of stromal TN-C on the adult urothelial transdifferentiation to prostatic epithelia in tissue recombination. AR-positive UGM has been demonstrated to induce the prostatic development and morphogen-

esis by action of androgens (Thompson et al., 1986). For example, UGM can induce prostatic epithelial development and morphogenesis in AR-negative endoderm-derived epithelia such as bladder and urethra (Cunha et al., 1983). The tissue recombinants composed of adult WT bladder urothelial cells and TN-C KO UGM showed that TN-C null UGM was not able to completely induce the bladder urothelial cells to undergo prostatic differentiation (Fig. 7). In addition, there was no prostatic secretion in the lumen. These results strongly suggest that stromal TN-C may play roles not only in prostatic epithelial cytodifferentiation but also in urothelial transdifferentiation to prostatic epithelia. Shima et al. (1995) previously reported that UGM-derived factors including growth factors and cytokines might regulate the epithelial cell differentiation in this process. Our results have proposed the idea that the adult urothelial transdifferentiation to prostatic epithelia requires ECM-signaling such as stromal TN-C.

Mature prostate tissue does not actively proliferate, and there is little cellular turnover in the adult prostate. It has been well known that mice do not spontaneously develop pathologic conditions such as BPH even in aged mouse prostate. However, several reports have shown prostatic epithelial hyperplasia in genetically modified mice. Mice carrying mutation of *Nkx3.1*, which is essential for normal morphogenesis and function of the prostate, showed prostatic epithelial hyperplasia and dysplasia (Bhatia-Gaur et al., 1999). In ERβ−/− mouse VP, there were increased epithelial proliferation, decreased apoptosis, and accumulation of incompletely differentiated cells, resulting in epithelial cellular hyperplasia (Imamov et al., 2004). The prostatic epithelium of PKS mice, which is a transgenic mouse with target overexpression of FGF-7/KGF in prostatic epithelium, was found to be hyperplastic (Foster et al., 2002). In TN-C KO mice, despite the significant increased mass of epithelial cell clusters and the number of binucleated cells (in AP and DLP), Ki-67 labeling indices of epithelial cells were very low in TN-C KO mice at 17 weeks and were similar to that of WT mice. In addition, there was no significant difference in apoptotic incidence at all stages examined.

In adult prostate of WT mice, TN-C is deposited along the stromal–epithelial interface. TN-C stimulates reorganization of actin stress fibers and disassembly of focal adhesion complexes, causing a weak adhesive state of the cells to the matrix (Murphy-Ullrich et al., 1991; Imanaka-Yoshida et al., 2001), which would facilitate changes of cell morphology. TN-C deficiency might make de-adhesion of the cells from the basement membrane difficult. The cells might become binucleated when mitosis without proper cytokinesis occurs (Stukenberg, 2004). In TN-C null condition, rigid adhesion of epithelial cells to the matrix could reduce the spontaneous detachment of the cells, resulting in multilayered epithelia following delayed turnover.

This study showed that deficiency of stromal TN-C signaling on mouse prostatic epithelium reduced or abolished expression of AR protein. An important feature of the normal adult prostate gland is the lack of proliferation even in the presence of growth-stimulating androgens. Ductal morphogenesis, epithelial cytodifferentiation, and proliferation/apoptosis are regulated by androgens acting through stromal AR, while epithelial AR is responsible for maintaining the differentiated phenotype and overall homeostasis of the glands (Hayward et al., 1997). Selective removal of AR signaling in luminal and basal epithelial cells stimulates mitogenesis and impaired functional differentiation in the growth quiescent adult prostate even though this effect was only seen late in life (Wu et al., 2007). In regard to cell adhesion, it is considered that rigid adhesion to basement membrane exerts a negative regulatory effect on AR expression and that the reduction in cell adhesion is a requirement for AR protein expression in the normal prostate epithelium (Knudsen and Miranti, 2006). Taken together with these findings, it is proposed that solid cell adhesion to the substratum caused by deficiency of de-adhesive molecule TN-C triggers loss of AR expression and cell differentiation in prostatic epithelium. Further investigation is necessary to determine the molecular mechanisms by which stromal TN-C deficiency induces multilayered, binucleated, and AR-negative ductal epithelial cells of the prostate.

Acknowledgments

We especially appreciate the advice and expertise of Drs. Teruyo Sakakura, Simon W. Hayward, Robert J. Matusik, and Neil A. Bhowmick. We also thank Mrs. Hiroko Nishii, Mari Hara, and Akiyo Sekimoto for technical support. This work was supported by Grants-in-Aid from the Ministry of Education for Science and Culture of Japan (17791072, 19591841, 19659412).

References

Bhatia-Gaur, R., Donjacour, A.A., Sciavolino, P.J., Kim, M., Desai, N., Young, P., Norton, C.R., Gridley, T., Cardiff, R.D., Cunha, G.R., Abate-Shen, C., Shen, M.M., 1999. Roles for Nkx3.1 in prostate development and cancer. Genes Dev. 13, 966–977.

Bhowmick, N.A., Chytil, A., Plieth, D., Gorska, A.E., Dumont, N., Shappell, S., Washington, M.K., Neilson, E.G., Moses, H.L., 2004. TGF-beta signaling in fibroblasts modulates the oncogenic potential of adjacent epithelia. Science 303, 848–851.

Chiquet-Ehrismann, R., Mackie, E.J., Pearson, C.A., Sakakura, T., 1986. Tenascin: an extracellular matrix protein involved in tissue interactions during fetal development and oncogenesis. Cell 47, 131–139.

Cunha, G.R., 1976. Epithelial–stromal interactions in development of the urogenital tract. Int. Rev. Cytol. 47, 137–194.

Cunha, G.R., Chung, L.W., Shannon, J.M., Reese, B.A., 1980. Stromal–epithelial interactions in sex differentiation. Biol. Reprod. 22, 19–42.

Cunha, G.R., Fujii, H., Neubauer, B.L., Shannon, J.M., Sawyer, L., Reese, B.A., 1983. Epithelial–mesenchymal interactions in prostatic development. I. Morphological observations of prostatic induction by urogenital sinus mesenchyme in epithelium of the adult rodent urinary bladder. J. Cell Biol. 96, 1662–1670.

El-Karef, A., Yoshida, T., Gabazza, E.C., Nishioka, T., Inada, H., Sakakura, T., Imanaka-Yoshida, K., 2007. Deficiency of tenascin-C attenuates liver fibrosis in immune-mediated chronic hepatitis in mice. J. Pathol. 211, 86–94.

Fata, J.E., Werb, Z., Bissell, M.J., 2004. Regulation of mammary gland branching morphogenesis by the extracellular matrix and its remodeling enzymes. Breast Cancer Res. 6, 1–11.

Forsberg, E., Hirsch, E., Frohlich, L., Meyer, M., Ekblom, P., Aszodi, A., Werner, S., Fassler, R., 1996. Skin wounds and severed nerves heal normally in mice lacking tenascin-C. Proc. Natl. Acad. Sci. U. S. A. 93, 6594–6599.

Foster, B.A., Evangelou, A., Gingrich, J.R., Kaplan, P.J., DeMayo, F., Greenberg, N.M., 2002. Enforced expression of FGF-7 promotes epithelial hyperplasia whereas a dominant negative FGFR2iiib promotes the emergence of neuroendocrine phenotype in prostate glands of transgenic mice. Differentiation 70, 624–632.

Fukamauchi, F., Wang, Y.J., Mataga, N., Kusakabe, M., 1997. Paradoxical behavioral response to apomorphine in tenascin-gene knockout mouse. Eur. J. Pharmacol. 338, 7–10.

Garrison, J.B., Kyprianou, N., 2004. Novel targeting of apoptosis pathways for prostate cancer therapy. Curr. Cancer Drug Targets 4, 85–95.

Green, K.A., Lund, L.R., 2005. ECM degrading proteases and tissue remodelling in the mammary gland. Bioessays 27, 894–903.

Hayward, S.W., Rosen, M.A., Cunha, G.R., 1997. Stromal–epithelial interactions in the normal and neoplastic prostate. Br. J. Urol. 79 (Suppl. 2), 18–26.

Ibrahim, S.N., Lightner, V.A., Ventimiglia, J.B., Ibrahim, G.K., Walther, P.J., Bigner, D.D., Humphrey, P.A., 1993. Tenascin expression in prostatic hyperplasia, intraepithelial neoplasia, and carcinoma. Hum. Pathol. 24, 982–989.

Imamov, O., Morani, A., Shim, G.J., Omoto, Y., Thulin-Andersson, C., Warner, M., Gustafsson, J.A., 2004. Estrogen receptor beta regulates epithelial cellular differentiation in the mouse ventral prostate. Proc. Natl. Acad. Sci. U. S. A. 101, 9375–9380.

Imanaka-Yoshida, K., Hiroe, M., Nishikawa, T., Ishiyama, S., Shimojo, T., Ohta, Y., Sakakura, T., Yoshida, T., 2001. Tenascin-C modulates adhesion of cardiomyocytes to extracellular matrix during tissue remodeling after myocardial infarction. Lab. Invest. 81, 1015–1024.

Imanaka-Yoshida, K., Matsumoto, K., Hara, M., Sakakura, T., Yoshida, T., 2003. The dynamic expression of tenascin-C and tenascin-X during early heart development in the mouse. Differentiation 71, 291–298.

Ingber, D.E., Folkman, J., 1989. How does extracellular matrix control capillary morphogenesis? Cell 58, 803–805.

Ishii, K., Shappell, S.B., Matusik, R.J., Hayward, S.W., 2005. Use of tissue recombination to predict phenotypes of transgenic mouse models of prostate carcinoma. Lab. Invest. 85, 1086–1103.

Knudsen, B.S., Miranti, C.K., 2006. The impact of cell adhesion changes on proliferation and survival during prostate cancer development and progression. J. Cell. Biochem. 99, 345–361.

Murphy-Ullrich, J.E., Lightner, V.A., Aukhil, I., Yan, Y.Z., Erickson, H.P., Hook, M., 1991. Focal adhesion integrity is downregulated by the alternatively spliced domain of human tenascin. J. Cell Biol. 115, 1127–1136.

Nakahara, H., Gabazza, E.C., Fujimoto, H., Nishii, Y., D'Alessandro-Gabazza, C.N., Bruno, N.E., Takagi, T., Hayashi, T., Maruyama, J., Maruyama, K., Imanaka-Yoshida, K., Suzuki, K., Yoshida, T., Adachi, Y., Taguchi, O., 2006. Deficiency of tenascin C

attenuates allergen-induced bronchial asthma in the mouse. Eur. J. Immunol. 36, 3334–3345.
Ohta, M., Sakai, T., Saga, Y., Aizawa, S., Saito, M., 1998. Suppression of hematopoietic activity in tenascin-C-deficient mice. Blood 91, 4074–4083.
Olumi, A.F., Grossfeld, G.D., Hayward, S.W., Carroll, P.R., Tlsty, T.D., Cunha, G.R., 1999. Carcinoma-associated fibroblasts direct tumor progression of initiated human prostatic epithelium. Cancer Res. 59, 5002–5011.
Orend, G., Chiquet-Ehrismann, R., 2006. Tenascin-C induced signaling in cancer. Cancer Lett. 244, 143–163.
Qian, J., Kumar, A., Szucsik, J.C., Lessard, J.L., 1996. Tissue and developmental specific expression of murine smooth muscle gamma-actin fusion genes in transgenic mice. Dev. Dyn. 207, 135–144.
Roth-Kleiner, M., Hirsch, E., Schittny, J.C., 2004. Fetal lungs of tenascin-C-deficient mice grow well, but branch poorly in organ culture. Am. J. Respir. Cell Mol. Biol. 30, 360–366.
Saga, Y., Yagi, T., Ikawa, Y., Sakakura, T., Aizawa, S., 1992. Mice develop normally without tenascin. Genes Dev. 6, 1821–1831.
Shima, H., Tsuji, M., Elfman, F., Cunha, G.R., 1995. Development of male urogenital epithelia elicited by soluble mesenchymal factors. J. Androl. 16, 233–241.
Shiraishi, T., Kato, H., Komada, S., Imai, H., Hirokawa, Y., Kusano, I., Yatani, R., Sakakura, T., 1994. Tenascin expression and postnatal development of the human prostate. Int. J. Dev. Biol. 38, 391–395.
Simian, M., Hirai, Y., Navre, M., Werb, Z., Lochter, A., Bissell, M.J., 2001. The interplay of matrix metalloproteinases, morphogens and growth factors is necessary for branching of mammary epithelial cells. Development 128, 3117–3131.
Stukenberg, P.T., 2004. Triggering p53 after cytokinesis failure. J. Cell Biol. 165, 607–608.
Sugimura, Y., Cunha, G.R., Donjacour, A.A., 1986. Morphogenesis of ductal networks in the mouse prostate. Biol. Reprod. 34, 961–971.
Takeda, H., Oike, Y., Sakakura, T., 1988. Immunofluorescent localization of tenascin during development of the mouse urogenital sinus: possible involvement in genital duct morphogenesis. Differentiation 39, 131–138.
Tamaoki, M., Imanaka-Yoshida, K., Yokoyama, K., Nishioka, T., Inada, H., Hiroe, M., Sakakura, T., Yoshida, T., 2005. Tenascin-C regulates recruitment of myofibroblasts during tissue repair after myocardial injury. Am. J. Pathol. 167, 71–80.
Thompson, H.G., Mih, J.D., Krasieva, T.B., Tromberg, B.J., George, S.C., 2006. Epithelial-derived TGF-beta2 modulates basal and wound-healing subepithelial matrix homeostasis. Am. J. Physiol. Lung Cell. Mol. Physiol. 291, L1277–L1285.
Thompson, T.C., Cunha, G.R., Shannon, J.M., Chung, L.W., 1986. Androgen-induced biochemical responses in epithelium lacking androgen receptors: characterization of androgen receptors in the mesenchymal derivative of urogenital sinus. J. Steroid. Biochem. 25, 627–634.
Tomas, D., Ulamec, M., Hudolin, T., Bulimbasic, S., Belicza, M., Kruslin, B., 2006. Myofibroblastic stromal reaction and expression of tenascin-C and laminin in prostate adenocarcinoma. Prostate Cancer Prostatic Dis. 9, 414–419.
Tremblay, L., Hauck, W., Nguyen, L.T., Allard, P., Landry, F., Chapdelaine, A., Chevalier, S., 1996. Regulation and activation of focal adhesion kinase and paxillin during the adhesion, proliferation, and differentiation of prostatic epithelial cells in vitro and *in vivo*. Mol. Endocrinol. 10, 1010–1020.
Tuxhorn, J.A., Ayala, G.E., Smith, M.J., Smith, V.C., Dang, T.D., Rowley, D.R., 2002. Reactive stroma in human prostate cancer: induction of myofibroblast phenotype and extracellular matrix remodeling. Clin. Cancer Res. 8, 2912–2923.
Vollmer, G., Michna, H., Ebert, K., Knuppen, R., 1994a. Androgen ablation induces tenascin expression in the rat prostate. Prostate 25, 81–90.
Vollmer, G., Michna, H., Schneider, M.R., Knuppen, R., 1994b. Stromal expression of tenascin is inversely correlated to epithelial differentiation of hormone dependent tissues. J. Steroid Biochem. Mol. Biol. 48, 487–494.
Weaver, V.M., Lelievre, S., Lakins, J.N., Chrenek, M.A., Jones, J.C., Giancotti, F., Werb, Z., Bissell, M.J., 2002. beta4 integrin-dependent formation of polarized three-dimensional architecture confers resistance to apoptosis in normal and malignant mammary epithelium. Cancer Cell. 2, 205–216.
Wu, C.T., Altuwaijri, S., Ricke, W.A., Huang, S.P., Yeh, S., Zhang, C., Niu, Y., Tsai, M.Y., Chang, C., 2007. Increased prostate cell proliferation and loss of cell differentiation in mice lacking prostate epithelial androgen receptor. Proc. Natl. Acad. Sci. U. S. A. 104, 12679–12684.
Xue, Y., Li, J., Latijnhouwers, M.A., Smedts, F., Umbas, R., Aalders, T.W., Debruyne, F.M., De La Rosette, J.J., Schalken, J.A., 1998. Expression of periglandular tenascin-C and basement membrane laminin in normal prostate, benign prostatic hyperplasia and prostate carcinoma. Br. J. Urol. 81, 844–851.

international journal of andrology ISSN 0105-6263

REVIEW ARTICLE

Developmental effects: oestrogen-induced vaginal changes and organotin-induced adipogenesis

T. Iguchi,* H. Watanabe,* Y. Ohta† and B. Blumberg‡

*Okazaki Institute for Integrative Bioscience, National Institute for Basic Biology, National Institutes of Natural Sciences, and Department of Basic Biology, Faculty of Life Science, Graduate University for Advanced Studies, Okazaki, Japan, †Department of Veterinary Science, Faculty of Agriculture, Tottori University, Tottori, Japan, and ‡Department of Developmental and Cell Biology, University of California Irvine, Irvine, CA, USA

Keywords:
adipogenesis, obesity, organotins, perinatal diethylstilbestrol exposure, peroxisome proliferator-activated receptor γ, retinoid X receptor α

Correspondence:
Taisen Iguchi, Division of Bio-Environmental Science, Department of Bio-Environmental Science, Okazaki Institute for Integrative Bioscience, National Institute for Basic Biology, National Institutes of Natural Sciences, 5-1 Higashiyama, Myodaiji, Okazaki Aichi 444-8787, Japan.
E-mail: taisen@nibb.ac.jp

Received 30 August 2007; revised 14 December 2007; accepted 18 December 2007

doi:10.1111/j.1365-2605.2008.00863.x

Summary

The emerging paradigm, the foetal origin of adult disease, is a new framework for considering the effects of endocrine disrupters on human and animal health. Prenatal diethylstilbestrol (DES) exposure resulted in various reproductive tract abnormalities in women, which is called as DES syndrome. Similar abnormalities have been demonstrated in experimental animals exposed perinatally to oestrogens. Developmental oestrogen exposure induces persistent proliferation of vaginal epithelial cells in mice. The persistent changes in the vagina of mice neonatally exposed to oestrogens results from persistent phosphorylation of erbB2 and oestrogen receptor α, sustained expression of EGF-like growth factors and phosphorylation of JNK1, IGF-I receptor and Akt. The ubiquitous environmental contaminant, tributyltin chloride (TBT) is well known to induce the development of male sex characteristics (imposex) in gastropods. We recently found that TBT and its congeners induce the differentiation of adipocytes in vitro and increase adipose mass in vivo in vertebrates. TBT is a nanomolar affinity ligand for retinoid X receptor (RXR) in the rock shell and for both the RXRα and the peroxisome proliferator-activated receptor γ (PPARγ) in the amphibian (*Xenopus laevis*) mouse, and human. TBT promotes adipogenesis in the murine 3T3-L1 cell model and perturbs key regulators of adipogenesis and lipogenic pathways in vivo, primarily through activation of RXRα and PPARγ. Moreover, *in utero* exposure to TBT leads to strikingly elevated lipid accumulation in adipose depots, liver, and testis of neonate mice and results in increased adipose mass in adults. In *X. laevis*, ectopic adipocytes form in and around gonadal tissues following organotin, RXRα or PPARγ ligand exposure. TBT represents the first example of an environmental endocrine disrupter that promotes adverse effects from gastropods to mammals. Prenatal (TBT) and early postnatal exposures (oestrogens) stand as strong examples of endocrine disrupting compounds that permanently alter developmental programming.

Introduction

Environmental endocrine-disrupting chemicals (EDCs) interact with steroid, arylhydrocarbon, retinoid and other nuclear receptors to regulate gene expression. Therefore, receptor-based functional assays are used in screening assays to detect biological activity of environmental chemicals (Iguchi *et al.*, 2006). Oestrogenic chemicals have been detected in aquatic environments worldwide and endocrine disruption in wild animals and humans exposed to EDCs during embryonic development has been summarized (Damstra *et al.*, 2002). Potentially new mechanisms for EDC action, such as proteasome-mediated degradation of receptors and their coregulators, genome-wide effects on DNA methylation status and modulation of lipid metabolism and adipogenesis, have recently been postulated (Tabb & Blumberg, 2006). Also, an emerging paradigm, the foetal origin of adult disease,

IJA 863 B
Journal Name | Manuscript No.
Dispatch: 8.1.08 | Journal: IJA | CE: Balaji Prasad
Author Received: | No. of pages: 6 | PE: Jeyachitra R

is a new framework for considering the effects of endocrine disruptors on human and animal health (Crews & McLachlan, 2006; Gluckman & Hanson, 2007). One example of this paradigm is the diethylstilbestrol (DES) syndrome. In humans, transplacental exposure to a synthetic oestrogen, DES, which was routinely prescribed to pregnant women for preventing miscarriages in 1940s–1970s, induces vaginal clear-cell adenocarcinoma and other reproductive tract abnormalities in young adult women (Herbst *et al.*, 1971; Herbst & Bern, 1981).

The perinatal mouse model has been used to understand molecular mechanism of the long-term effects of early exposure to oestrogenic chemicals exposure on the female reproductive tract (Herbst & Bern, 1981; Iguchi, 1992, 2000; McLachlan, 2001). Neonatal treatment of female mice with oestradiol (E2), DES, or the xenoestrogen, bisphenol A induces abnormalities in the reproductive tracts, hypothalamo-hypophysial-ovarian axis, immune system, and skeletal and muscular tissues (Newbold, ????; Iguchi *et al.*, 2002). The growth response of perinatally DES-exposed reproductive organs to oestrogen is altered, as are levels of oestrogen receptors (ER), epidermal growth factor receptor, prolactin receptor, oncogenes and *Hox* genes (Yin & Ma, 2005; Iguchi *et al.*, 2006).

Organotins are a diverse group of widely distributed environmental pollutants. Tributyltin chloride (TBT) and bis(triphenyltin) oxide (TPT) cause multiple adverse effects on the invertebrate and vertebrate endocrine systems. Organotins were introduced as antifouling agents in marine shipping paints in the 1960s. Although the use of TBT in antifouling paints has been restricted, organotins continue to occur as contaminants in dietary sources, such as fish and shellfish, and through their use as pesticides and fungicides on food crops (Golub & Doherty, ????). Humans are also exposed to organotins through their use in wood treatments, industrial water systems and textiles. Mono- and di-organotins are used as stabilizers in the manufacture of polyvinyl chloride plastics, which introduces the potential for transfer by contact with drinking water and foods.

TBT-induced imposex (the superimposition of male sex characteristics on female gastropod molluscs) represents one of the most clear-cut examples of environmental endocrine disruption because effects occur at the doses to which organisms are exposed (reviewed in Iguchi *et al.*, 2007). Imposex impairs reproduction in severely affected animals, resulting in significant population declines. TBT exposure also leads to masculinization of two fish species but TBT exposure has only been shown to result in slight effects on the mammalian reproductive tracts; no reports of altered sex ratios have been forthcoming (see Iguchi *et al.*, 2007). Hepatic-, neuro- and immunotoxicity were reported to be the major effects of organotin exposure in mammals; immunotoxicity is the primary regulatory endpoint for TBT exposure (Boyer, 1989). Current understanding of how organotins disrupt the endocrine system is based on the ability of organotins to modulate the expression or activity of steroid regulatory enzymes and via less specific toxic effects secondary to mitochondrial damage (Powers & Beavis, 1991; Gennari *et al.*, 2000; Cooke, 2002). These data do not permit one to draw firm conclusions regarding whether organotins function primarily as protein and enzyme inhibitors in vivo, or instead regulate gene expression in a more direct manner.

This review examines the emerging paradigm, the foetal origin of adult disease, in which prenatal, or early postnatal exposure to environmental chemicals leads to permanent phenotypic changes, irrespective of subsequent exposure. This 'foetal origins of disease' model provides important insights into the aetiology of chronic diseases. It has considerable support from epidemiological studies (Gluckman & Hanson, 2007), but much less in terms of molecular details. We discuss two model systems for which molecular mechanisms are becoming clear: the induction of persistent vaginal proliferation in neonatally oestrogen-exposed mouse vagina and the role of environmental obesogens in adipogenesis, focusing on changes in gene expression that may be responsible for the effects observed.

Persistent vaginal changes induced by perinatal oestrogen exposure

Long-term oestrogen stimulation is a known risk factor for carcinogenesis in laboratory animals and humans (Marselos & Tomatis, 1992a,b). In humans, transplacental exposure to DES, a synthetic oestrogen prescribed to pregnant women for preventing miscarriages, induced vaginal clear-cell adenocarcinoma and other reproductive tract abnormalities in young adult women (Herbst *et al.*, 1971; Herbst & Bern, 1981). As generation of women exposed to DES approach menopause, concern has arisen about their health risk, because it has been hypothesized that in utero DES exposure influences the incidences of breast cancer, squamous neoplasia of the cervix and vagina, and vaginal clear-cell adenocarcinoma later in life (Herbst, 2000; Hatch *et al.*, 2001; Palmer *et al.*, 2002). Rodent models of DES exposure have been developed to understand the mechanistic basis of DES effects in humans. In mice, developmental exposure to oestrogens including DES elicits various permanent alterations in female reproductive tracts. For example, in the vagina, neonatal oestrogen administration induces persistent cell proliferation and cornification of vaginal epithelium even after ovariectomy, resulting in hyperplastic cancerous

lesions later in life (Newbold, ????; Takasugi *et al.*, 1962; Forsberg, 1979; McLachlan *et al.*, 1980; Herbst & Bern, 1981; Iguchi, 1992, 2000; McLachlan, 2001). This rodent model, which stimulates the effects of developmental DES exposure in humans, has been characterized, yet the underlying mechanisms remain poorly understood. This irreversible proliferation and differentiation of the vaginal epithelium may be attributable to oestrogen-independent, persistent activation of downstream growth factor expression. Indeed, high levels of EGF, TGF-α and other genes are expressed in the vaginae of DES-treated mice, even after ovariectomy (Nelson *et al.*, 1994; Takahashi *et al.*, 1994; Sato *et al.*, 2004). Therefore, we analysed the role of crosstalk between erbB signalling and ER in oestrogen-independent effects induced by neonatal DES using mouse vagina.

Persistent phosphorylation of erbB2, EGF receptor and ERα, and sustained expression of EGF-like growth factors and phosphorylation of JNK1, IGF-I receptor and Akt, occurs in the vagina of neonatally oestrogen-exposed mice (Miyagawa *et al.*, 2004). DNA microarray analysis of the neonatally DES-exposed mouse vagina showed that expression patterns of genes related to cellular signalling were altered. We also found high expression of interleukin-1-related genes accompanied by phosphorylation of JNK1. Expression of IGF-1 and its binding proteins was modulated and led to phosphorylation of IGF-1 receptor and Akt, which is one of the downstream factors of IGF-1 signalling (Miyagawa *et al.*, 2004) (Fig. 1). In order to understand the molecular basis of the critical period of DES-induced vaginal changes, patterns of gene expression

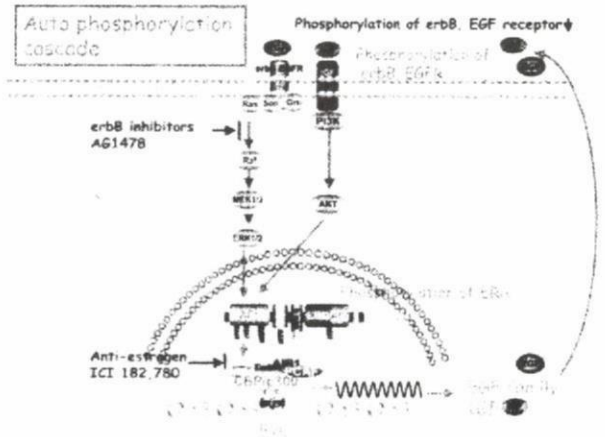

Figure 1 Possible mechanism of persistent proliferation of mouse vaginal epithelial cells induced by perinatal exposure to oestrogens including diethylstilbestrol (DES). Auto-stimulation cascade has been established in the mouse vaginal epithelial cells exposed perinatally to DES: persistently expressed EGF-related growth factors and IGF-1 induced persistent phosphorylation of oestrogen receptor α, erbB2, EGF receptor and IGF-1 receptor.

induced by DES were analysed using DNA microarrays. The number of DES-induced genes during the critical period, PND 0, was smaller than those found after the critical period (Suzuki *et al.*, 2006). In utero DES exposure induced changes in expression of genes such as DKK2, Nkd2 and sFRP1 as well as changes in genes of the Wnt and Eph families in the female reproductive tracts. The genes could be the basis for various reproductive tract abnormalities following exposure to DES (Suzuki *et al.*, 2007). Also, prenatal DES exposure resulted in altered methylation of specific genes (Li *et al.*, 2003). The epigenetic changes may lead to altered gene expression and hence to altered tissue function, which may produce increased susceptibility to disease and dysfunction later in life (Heindel & Lawler, 2007). Therefore, analysis of methylation status of genes showing altered expression in the mouse vagina is underway.

Adipogenesis stimulation by organotins in vertebrates

The conventional wisdom suggests that high calorie modern diets, coupled with reduced physical activity are the major, if not the only cause of the rising worldwide incidence of obesity (Hill & Peters, 1998). Although the role played by genetic components is not completely clear, there is little doubt that genetic variation affects individual weight gain. However, it is difficult to imagine a scenario where genetic variation could underlie the rapid worldwide increase in obesity. It is more reasonable to suggest that interaction with the modern environment exposes underlying genetic differences that affect obesity. The Barker hypothesis postulates that in utero foetal nutritional status is a potential risk factor for obesity and related diseases (Baker *et al.*, 1990, 1993; Phillips *et al.*, 1994; Martyn *et al.*, 1995; Yajnik, 2000). Developmental programming of a thrifty phenotype limits the range of subsequent responses to environmental factors such as diet and exercise (Lucas, 1998). Experiments in animal models support this hypothesis (Armitage *et al.*, 2004). Plausible mechanisms include imprinting of obesity-sensitive hormonal pathways or changes in cell type and number, e.g. adipocytes, established during development. One such developmental programming event could be exposure to xenobiotic chemicals which are becoming increasingly prevalent in the environment. Our environmental 'obesogen' model predicted the existence of xenobiotic chemicals that inappropriately regulate lipid metabolism and adipogenesis to promote obesity (Grün & Blumberg, 2006; Grün *et al.*, 2006).

Recent work has shown that aromatase mRNA levels are down-regulated in human ovarian prolifera cells by treatment with organotins or ligands for the nuclear hormone

receptors, RXR or peroxisome proliferator-activated receptor γ (PPARγ) (de Souza *et al.*, 2001; Kanayama *et al.*, 2005; Nakanishi *et al.*, 2005; Grün & Blumberg, 2006; Grün *et al.*, 2006). In the gastropod *Thais clavigera* RXR homolog is responsive to 9-*cis* RA and TBT, and 9-*cis* RA can also induce imposex (reviewed in Iguchi *et al.*, 2007). We found similar effects of TBT and RXR/PPARγ ligands on mammalian aromatase mRNA expression intriguing and hypothesized that TBT might exert some of its biological effects as a transcriptional regulation of gene expression. Accordingly, we tested the ability of TBT to activate a panel of nuclear receptors.

The results show that TBT is a high-affinity ligand for RXRα and PPARγ and induces adipogenesis in cultured cells and in animal models (Kanayama *et al.*, 2005; Grün & Blumberg, 2006; Grün *et al.*, 2006). Several organotins activated both receptors. Remarkably, organotins of relatively diverse 3-D structures (e.g. TBT and TPT) are efficient activators and ligands for these receptors. The strong binding affinity of organotins for the receptors, taken together with the ability of organotins to compete with high-affinity RXR and PPAR ligands for receptor binding, suggest that organotins are bona fide ligands for both RXRs and PPARγ. TBT activates both receptors at nanomolar concentrations, far below the micromolar levels at which other mechanisms of toxicity become apparent.

The RXRα–PPARγ heterodimer is a master regulator of adipocyte differentiation and lipid storage; it also directly regulates lipid metabolism. Activation of PPARγ by TBT or specific ligands promotes the expression of genes that increase fatty acid storage and inhibits expression of genes that induce lipolysis (Grün & Blumberg, 2006; Grün *et al.*, 2006) (Fig. 2). Prenatal exposure to TBT led to persistent changes in the exposed animals such that they became 15% heavier later in life (Grün & Blumberg, 2006). This is consistent with the increased body fat mass observed in patients treated with antidiabetic thiazolidinediones that act through PPARγ to increase triglyceride storage in adipocytes and increase adipocyte numbers (de Souza *et al.*, 2001). The ability of thiazolidinediones to increase adipocyte number and fat mass suggests that TBT exposure could affect obesity at any time in life. We are currently investigating whether TBT treatment induces increased fat mass by increasing the number of adipocyte precursors, enhancing adipocyte differentiation from the same number of precursors, promoting proliferation of mesenchymal stem cells that become fat cells, or some combination of these.

Conclusion

Two models of 'foetal origins of disease' are provided. Developmental exposure of oestrogens including DES induces persistent proliferation of mouse vaginal epithelium, which is accompanied by persistent phosphorylation of erbB2 and ERα, sustained expression of EGF-like growth factors, and phosphorylation of JNK1, IGF-I receptor and Akt. Organotins such as TBT and TPT act as RXR activators, resulting in the development of imposex in the rock shell. They also act as chemical stressors or 'obesogens' that activate RXR and PPARγ signalling to promote long-term changes in adipocyte number and/or lipid homeostasis following developmental or chronic lifetime exposure in vertebrates.

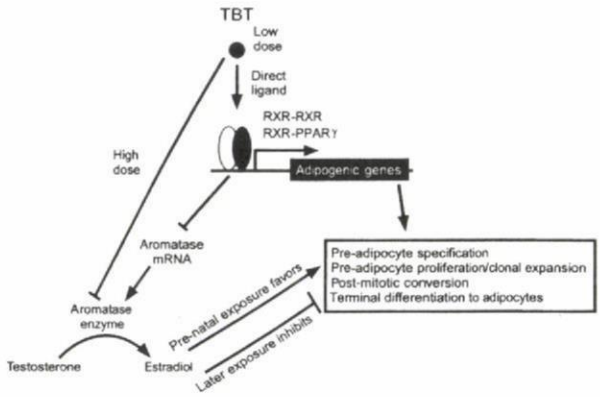

Figure 2 TBT action on nuclear receptors. Highly schematic and abbreviated version of known sites of TBT action that may impact sex determination or adipogenesis. At low (nanomolar) doses, TBT acts as a high-affinity ligand for RXR and PPARγ. It can activate RXR–PPARγ target genes involved in adipogenesis as shown. RXR–PPARγ heterodimers are also known to transcriptionally downregulate the expression of aromatase mRNA, thereby reducing the available levels of aromatase enzyme. Decreased enzyme levels lead to increased testosterone and decreased oestradiol levels. At high doses, TBT can also inhibit aromatase enzymatic activity, causing the same result.

Acknowledgements

Partly supported by grants from the Ministry of Education, Culture, Sports, Science and Technology of Japan; Ministry of the Environment of Japan; Ministry of Health Labour and Welfare of Japan (to T.I.), and grants from the U.S. Environmental Protection Agency (STAR R830686) and National Institutes of Health (GM-60572) (to B.B.).

References

Armitage, J. A., Khan, I. Y., Taylor, P. D., Nathanielsz, P. W. & Poston, L. (2004) Developmental programming of metabolic syndrome by maternal nutritional imbalance; how strong is the evidence from experimental models in mammals? *Journal of Physiology* 561, 355–377.

Baker, D. J., Bull, A. R., Osmond, C. & Simmonds, S. J. (1990) Fetal and placental size and risk of hypertension in adult life. *British Medical Journal* 301, 259–262.

Baker, D. J., Martyn, C. N., Osmond, C., Hales, C. N. & Fall, C. H. (1993) Growth in utero and serum cholesterol concentrations in adult life. *British Medical Journal* 307, 1524–1527.

Boyer, I. J. (1989) Toxicity of dibutyltin, tributyltin and other organotin compounds to humans and to experimental animals. *Toxicology* 55, 253–298.

Cooke, G. M. (2002) Effect of organotins on human aromatase activity in vitro. *Toxicology Letters* 126, 121–130.

Crews, D. & McLachlan, J. A. (2006) Epigenetics, evolution, endocrine disruption, health, and disease. *Endocrinology* 147, S4–S10.

Damstra, T., Barlow, S., Bergman, A., Kavlock, R. & van der Kraak, G. (2002) Global Assessment of the State-of-the-Science of Endocrine Disruptors, p. 180. International Programme on Chemical Safety, World Health Organization, Geneva.

Forsberg, J.-G. (1979) Developmental mechanism of estrogen-induced irreversible changes in the mouse cervicovaginal epithelium. *National Cancer Institute Monograph* 51, 41–56.

Gennari, A., Viviani, B., Galli, C. L., Marinovich, M., Pieters, R. & Corsini, E. (2000) Organotins induce apoptosis by disturbance of $[Ca^{2+}]$ and mitochondrial activity, causing oxidative stress and activation of caspases in rat thymocytes. *Toxicology and Applied Pharmacology* 169, 185–190.

Gluckman, P. D. & Hanson, M. A. (eds) (2007) Developmental Origin of Health and Disease, p. 519. Cambridge University Press, ????.

Golub, M. & Doherty, J. (????) Triphenyltin as a potential human endocrine disruptor. *Journal of Toxicology and Environmental Health. Part B, Critical Reviews* 7, 282–295.

Grün, F. & Blumberg, B. (2006) Environmental obesogens: organotins and endocrine disruption via nuclear receptor signaling. *Endocrinology* 147, S50–S55.

Grün, F., Watanabe, H., Zamanian, Z., Maeda, L., Arima, K., Chubacha, R., Gardiner, D. M., Kanno, J., Iguchi, T. & Blumberg, B. (2006) Endocrine disrupting organotin compounds are potent inducers of adipogenesis in vertebrates. *Molecular Endocrinology* 20, 2141–2155.

Hatch, E. E., Herbst, A. L., Hoover, R. N., Noller, K. L., Adam, E., Kaufman, R. H. *et al.* (2001) Incidence of squamous neoplasia of the cervix and vagina in women exposed prenatally to diethylstilbestrol (United States). *Cancer Causes and Control* 12, 837–845.

Heindel, J. & Lawler, C. (2007) Role of exposure to environmental chemicals in developmental origins of health and disease. In: Developmental Origins of Health and Disease (eds P. Gluckman & M. Hanson), pp. 82–97. Cambridge Univ. Press, Cambridge, UK.

Herbst, A. L. (2000) Behavior of estrogen-associated female genital tract cancer and its relation to neoplasia following intrauterine exposure to diethylstilbestrol (DES). *Gynecologic Oncology* 76, 147–156.

Herbst, A. L. & Bern, H. A. (eds.) (1981) Developmental Effects of Diethylstilbestrol (DES) in Pregnancy, p. 203. Thieme Stratton Inc., New York.

Herbst, A. L., Ulfelder, H. & Poskanzer, D. C. (1971) Adenocarcinoma of the vagina. Association of maternal stilbestrol therapy with tumor appearance in young women. *The New England Journal of Medicine* 284, 878–881.

Hill, J. O. & Peters, J. C. (1998) Environmental contributions to the obesity epidemic. *Science* 280, 1371–1374.

Iguchi, T. (1992) Cellular effects of early exposure to sex hormones and antihormones. *International Review of Cytology* 139, 1–57.

Iguchi, T. (2000) Embryonic and neonatal exposure to endocrine-altering contaminants: effects on mammalian female reproduction. In: Environmental Endocrine Disrupters (eds L. Guillette Jr & D. A. Crain), pp. 234–268. Taylor & Francis, New York.

Iguchi, T., Watanabe, H., Katsu, Y., Mizutani, T., Miyagawa, S., Suzuki, A., Sone, K. & Kato, H. (2002) Developmental toxicity of estrogenic chemicals on rodents and other species. *Congenital Anomalies* 42, 94–105.

Iguchi, T., Irie, F., Urushitani, H., Tooi, O., Kawashima, Y., Roberts, M., Norrgren, L. & Hutchinson, T. H. (2006a) Availability of *in vitro* vitellogenin assay for screening of estrogenic and anti-estrogenic activities of environmental chemicals. *Environmental Sciences* 13, 161–183.

Iguchi, T., Watanabe, H. & Katsu, Y. (2006b) Application of ecotoxicogenomics for studying endocrine disruption in vertebrates and invertebrates. *Environmental Health Perspectives* 114(Suppl. 1), 101–105.

Iguchi, T., Katsu, Y., Horiguchi, T., Watanabe, H., Blumberg, B. & Ohta, Y. (2007) Endocrine disrupting organotin compounds are potent inducers of imposex in gastropods and adipogenesis in vertebrates. *Molecular and Cell Toxicology*, 3, 1–10.

Kanayama, T., Kobayashi, N., Mamiya, S., Nakanishi, T. & Nishikawa, J. (2005) Organotin compounds promote adipocyte differentiation as agonists of the peroxisome proliferator-activated receptor gamma/retinoid X receptor pathway. *Molecular Pharmacology* 67, 766–774.

Li, S., Hansman, R., Newbold, R. R., Davis, B. & McLachlan, J. (2003) Neonatal diethylstilbestrol exposure induces persistent elevation of c-fos expression and hypomethylation of its exon-4 in mouse uterus. *Molecular Carcinogenesis* 38, 78–84.

Lucas, A. (1998) Programming by early nutrition: an experimental approach. *Journal of Nutrition* 128, 401S–406S.

Marselos, M. & Tomatis, L. (1992a) Diethylstilbestrol: I, pharmacology, toxicology and carcinogenicity in humans. *European Journal of Cancer* 28A, 1182–1189.

Marselos, M. D. & Tomatis, L. (1992b) Diethylstilbestrol : II, pharmacology, toxicology and carcinogenicity in experimental animals. *European Journal of Cancer* 29A, 149–155.

Martyn, C. N., Barker, D. J., Jespersen, S., Greenwald, S., Osmond, C. & Berry, C. (1995) Growth in utero, adult blood pressure, and arterial compliance. *British Heart Journal* 73, 116–121.

McLachlan, J. A. (2001) Environmental signaling: what embyos and evolution teach us about endocrine disrupting chemicals. *Endocrine Reviews* 22, 319–341.

McLachlan, J. A., Newbold, R. R. & Bullock, B. C. (1980) Long-term effects on the female mouse genital tract associated with prenatal exposure to diethylstilbestrol. *Cancer Research* 40, 3988–3999.

Miyagawa, S., Katsu, Y., Watanabe, H. & Iguchi, T. (2004a) Estrogen-independent activation of ErbBs signaling and estrogen receptor α in the mouse vagina exposed neonatally to diethylstilbestrol. *Oncogene* 23, 340–349.

Miyagawa, S., Suzuki, A., Katsu, Y., Kobayashi, M., Goto, M., Handa, H., Watanabe, H. & Iguchi, T. (2004b) Persistent gene expression in mouse vagina exposed neonatally to diethylstilbestrol. *Journal of Molecular Endocrinology* 32, 663–677.

Nakanishi, T., Nishikawa, J., Hiromori, Y., Yokoyama, H., Koyanagi, M., Takasuga, S. *et al.* (2005) Trialkyltin compounds bind retinoid X receptor to alter human placental endocrine functions. *Molecular Endocrinology* 19, 2502–2516.

Nelson, K. G., Sakai, Y., Eitzman, B., Steed, T. & McLachlan, J. (1994) Exposure to diethylstilbestrol during a critical developmental period of the mouse reproductive tract leads to persistent induction of two estrogen-regulated genes. *Cell Growth and Differentiation* 5, 595–606.

Newbold, R. R. (????) Lessons learned from perinatal exposure to diethylstilbestrol. *Toxicology and Applied Pharmacology* 199, 142–150.

Palmer, J. R., Hatch, E. E., Rosenberg, C. L., Hartge, P., Kaufman, R. H., Titus-Ernstoff, L. *et al.* (2002) Risk of breast cancer in women exposed to diethylstilbestrol *in utero*: preliminary results (United States). *Cancer Causes and Control* 13, 753–758.

Phillips, D. I., Hirst, S., Clark, P. M., Hales, C. N. & Osmond, C. (1994) Fetal growth and insulin secretion in adult life. *Diabetologia* 37, 592–596.

Powers, M. F. & Beavis, A. D. (1991) Triorganotins inhibit the mitochondrial inner membrane anion channel. *Journal of Biological Chemistry* 266, 17250–17256.

Sato, T., Fukazawa, Y., Ohta, Y. & Iguchi, T. (2004) Involvement of growth factors in induction of persistent proliferataion of vaginal epithelium of mice exposed neonatally to diethylstilbestrol. *Reproductive Toxicology*, 19, 43–51.

de Souza, C. J., Eckhardt, M., Gagen, K., Dong, M., Chen, W., Laurent, D. & Burkey, B. F. (2001) Effects of pioglitazone on adipose tissue remodeling within the setting of obesity and insulin resistance. *Diabetes* 50, 1863–1871.

Suzuki, A., Watanabe, H., Mizutani, T., Sato, T., Ohta, Y. & Iguchi, T. (2006) Global gene expression in mouse vaginae exposed to diethylstilbestrol at different ages. *Experimental Biology and Medicine* 231, 632–640.

Suzuki, A., Urushitani, H., Sato, T., Watanabe, H., Ohta, Y. & Iguchi, T. (2007) Gene expression change in the Müllerian duct of the mouse fetus exposed to diethylstilbestrol *in utero*. *Experimental Biology and Medicine* 232, 503–514.

Tabb, M. M. & Blumberg, B. (2006) New modes of action for endocrine-disrupting chemicals. *Molecular Endocrinology* 20, 475–482.

Takahashi, T., Eitzman, B., Bossert, N. L., Walmer, D., Sparrow, K., Flanders, K. C., McLachlan, J. & Nelson, K. G. (1994) Transforming growth factors beta 1, beta 2, and beta 3 messenger RNA and protein expression in mouse uterus and vagina during estrogen-induced growth: a comparison to other estrogen-regulated genes. *Cell Growth and Differentiation* 5, 919–935.

Takasugi, N., Bern, H. A. & DeOme, K. (1962) Persistent vaginal cornification in mice. *Science* 138, 438–439.

Yajnik, C. (2000) Interactions of perturbations in intrauterine growth and growth during childhood on the risk of adult-onset disease. *Proceedings of the Nutrition Society* 59, 257–265.

Yin, Y. & Ma, L. (2005) Development of the mammalian female reproductive tract. *Journal of Biochemistry* 137, 677–683.

Activation of Steroid and Xenobiotic Receptor (SXR, NR1I2) and Its Orthologs in Laboratory, Toxicologic, and Genome Model Species

Matthew R. Milnes,[1,] Adriana Garcia,[1] Emily Grossman,[1] Felix Grün,[1] Jason Shiotsugu,[1] Michelle M. Tabb,[1,**] Yukio Kawashima,[2] Yoshinao Katsu,[3] Hajime Watanabe,[3] Taisen Iguchi,[3] and Bruce Blumberg[1]*

[1]Department of Developmental and Cell Biology, University of California, Irvine, California, USA; [2]Japan NUS Co. Ltd., Tokyo, Japan; [3]Okazaki Institute for Integrative Bioscience, National Institute for Basic Biology, National Institutes of Natural Sciences, Okazaki, Japan

Background: Nuclear receptor subfamily 1, group I, member 2 (NR1I2), commonly known as steroid and xenobiotic receptor (SXR) in humans, is a key ligand-dependent transcription factor responsible for the regulation of xenobiotic, steroid, and bile acid metabolism. The ligand-binding domain is principally responsible for species-specific activation of NR1I2 in response to xenobiotic exposure.

Objectives: Our objective in this study was to create a common framework for screening NR1I2 orthologs from a variety of model species against environmentally relevant xenobiotics and to evaluate the results in light of using these species as predictors of xenobiotic disposition and for assessment of environmental health risk.

Methods: Sixteen chimeric fusion plasmid vectors expressing the Gal4 DNA-binding domain and species-specific NR1I2 ligand-binding domain were screened for activation against a spectrum of 27 xenobiotic compounds using a standardized cotransfection receptor activation assay.

Results: NR1I2 orthologs were activated by various ligands in a dose-dependent manner. Closely related species show broadly similar patterns of activation; however, considerable variation to individual compounds exists, even among species varying in only a few amino acid residues.

Conclusions: Interspecies variation in NR1I2 activation by various ligands can be screened through the use of *in vitro* NR1I2 activation assays and should be taken into account when choosing appropriate animal models for assessing environmental health risk.

Key words: endocrine disruption, metabolism, pesticides, phthalates, PXR, SXR, xenobiotics. *Environ Health Perspect* 116:880–885 (2008). doi:10.1289/ehp.10853 available via *http://dx.doi.org/* [Online 12 March 2008]

The ability of a xenobiotic substance to induce protection against subsequent exposure and also to induce protection against exposure to other potentially toxic compounds was first described more than 30 years ago by Hans Selye (1971). It was quickly realized that such "catatoxic" compounds led to an increase in hepatic cytochrome P450 (CYP) enzyme activity (Einarsson and Gustafsson 1973) and that the substrates of the activated enzymes were relatively nonspecific. In 1998, activation of human CYP3A4 was shown to be primarily mediated by nuclear receptor subfamily 1, group I, member 2 [NR1I2; GenBank accession no. AY091855; National Center for Biotechnology Information (NCBI) 2007b]. For purposes of clarification, we use the trivial names of NR1I2 orthologs associated with specific taxonomic groups. This receptor is commonly known as the steroid and xenobiotic receptor (SXR) in primates (Blumberg et al. 1998), pregnane X receptor (PXR) in nonprimate mammals (Kliewer et al. 1998; Lehmann et al. 1998), chicken X receptor (CXR) in birds (Moore et al. 2002), and benzoate X receptor (BXR) in amphibians (Grün et al. 2002). It is now well established that the most prevalent CYP enzymes in the liver, members of the CYP3A and 2B subfamilies, along with a host of conjugating enzymes and ATP binding cassette (ABC) family membrane transport proteins, are under direct transcriptional regulation by NR1I2 (Xie et al. 2000b, 2004).

Through the action of its target genes, NR1I2 is a key regulator of bile salt, steroid hormone, and xenobiotic metabolism and excretion (Kliewer et al. 2002). NR1I2 is a member of the nuclear hormone receptor superfamily, which also includes sex steroid receptors, thyroid receptor, and other orphan receptors such as constitutive androstane receptor (CAR, NR1I3). The term "orphan receptor" has been given to a number of transcription factors that are related to nuclear receptors but for which a definitive endogenous ligand was not initially identified. Ligand-dependent activation of NR1I2 is mediated by steroid hormones, dietary compounds (e.g., phytoestrogens), vitamins E and K, medicinal herbs, xenobiotics, and approximately 50% of prescription drugs (reviewed by Dussault and Forman 2002; Kretschmer and Baldwin 2005). These ligands are extremely varied in chemical structure and application, and some have been shown to activate or antagonize NR1I2 orthologs in a species-specific manner (e.g., rifampicin, coumestrol, highly chlorinated polychlorinated biphenyls) (Blumberg et al. 1998; Jones et al. 2000; Tabb et al. 2004).

Development of the so-called humanized mouse was an important step in understanding the pharmacology of xenobiotic metabolism (Xie et al. 2000a). This animal is deficient in the rodent NR1I2 ortholog, PXR, and transgenic for human SXR expression in the liver. This model demonstrates convincingly that NR1I2 is the key regulator of CYP3A expression and that selective activation of target genes in response to species-specific activators depends on the ligand-binding domain (LBD) of this receptor, rather than on the DNA-binding domain (DBD) or target DNA-binding elements. The primary sequence of the LBD for NR1I2 varies greatly across species. The sequence similarity can be as low as 75% between mammalian NR1I2 orthologs and as low as 49% when comparing the chicken ortholog, CXR, to human SXR (Moore et al. 2002). A fundamental assumption made when using the results of model animal experiments to predict effects on humans or wildlife is that uptake and metabolism of the compound as well as the biochemistry and endocrinology of the organism is similar between the model species and species of concern. In some cases, the response of a model species to chemical exposure is reasonably predictive of the effects on humans. In other cases, the connection is more uncertain,

Address correspondence to B. Blumberg, Department of Developmental and Cell Biology, University of California, 5205 McGaugh Hall, Irvine, CA 92697-2300 USA. Telephone: (949) 824-8573. Fax: (949) 824-4709. E-mail: blumberg@uci.edu

*Current address: Conservation and Research for Endangered Species, Zoological Society of San Diego, Escondido, California, USA.

**Current address: Focus Diagnostics, Cypress, California, USA.

We thank J. Ycaza for assistance with plasmid preparations.

This study was supported by grants from the U.S. Environmental Protection Agency (STAR-CR830686) and an unrestricted research gift from Eisai Co, Ltd. to B.B.; Grants-in-Aid for Scientific Research from the Ministry of Education, Culture, Sports, Science and Technology of Japan; a Health Sciences Research Grant from the Ministry of Health, Labour and Welfare, Japan, and a grant from the Ministry of Environment, Japan, to T.I. M.R.M. was supported by an institutional training grant from the National Institutes of Health (CA09054-29) and a University of California President's Postdoctoral Fellowship.

B.B. is a named inventor on U.S. patents related to SXR (6,756,491, 6,809,178, and 6,984,773). The Salk Institute for Biological Studies (La Jolla, CA), which has licensed them to various for-profit entities, controls these patents. The remaining authors declare they have no competing financial interests.

Received 5 September 2007; accepted 11 March 2008.

and the ability to predict risk is not reliable. Understanding how the xenobiotic response differs among species is essential to developing high-quality models and characterizations of risk from chemical exposure.

The goal of this study was to screen a wide variety of xenobiotic compounds for interaction with NR1I2 orthologs within a common system, thus providing the framework for understanding the metabolism of xenobiotics in different model species. To compare responses correlating to interspecies variation in the LBD of NR1I2, we used an *in vitro* luciferase reporter assay driven by yeast Gal4 DBD-NR1I2 LBD fusion plasmids. Advantages of this system are that it eliminates the need to clone each species' bona fide response and is insensitive to induction by endogenous receptors. One disadvantage of this system is that it is insensitive to interspecies variation in activation function-1 (AF-1) region coregulator recruitment; however, the availability of coregulators in any *in vitro* system is not necessarily representative of the *in vivo* environment. A structurally diverse array of xenobiotics was chosen (Table 1) to represent a broad spectrum of chemical classes and applications that published data indicate are of considerable environmental and/or health concern. NR1I2 orthologs tested included commonly used laboratory, toxicologic, and/or genome model species. The results of these experiments have important implications for determining the appropriate use of animal models and for assessing whether we can reasonably rely on those models to predict results in other species, including humans.

Materials and Methods

Cloning of NR1I2 orthologs. LBD coding sequence has previously been reported in GenBank for NR1I2 orthologs in human (accession no. AY091855), dog (AF454670), rabbit (AF182217), rat (AF151377), mouse (NM010936), chicken (AF276753), *Xenopus laevis* BXRα (BC041187) and BXRβ (AF305201), and zebrafish (AF502918). Novel NR1I2 LBD sequences were cloned from Japanese macaque (*Macaca fuscata*), crab-eating macaque (*Macaca fascicularis*), marmoset (*Callithrix jacchus*), quail (*Coturnix japonica*), fathead minnow (*Pimephales promelas*), fugu (*Takifugu rubripes*), and medaka (*Oryzias latipes*). For novel sequences, optimized degenerate primers (forward 5′-AGAACTAGTG-GATCCGYGARGGNTGYAARGGNTTYT T and reverse 5′-GGTATCGATAAGCTTG-CYTGCATNARNACRTAYTCYTC) were used for polymerase chain reaction (PCR) amplification of a region extending from the first zinc finger of the DBD (C E G C K G F F) into the LBD (E E Y V L M Q A) for each species. We used nested primers derived from the amplified region and 3′-RACE (rapid amplification of cDNA ends) to obtain full LBD sequences beginning with the coding region corresponding to human SXR Met-107 from liver cDNA libraries from each species. Gal4-NR1I2 fusion constructs were created by subcloning the LBD into *Eco*RI and *Bam*HI sites of the vector pCMX-Gal4N (Blumberg et al. 1998) using *Exo*III-mediated ligation-independent cloning (Li and Evans 1997). The PCR products were directly sequenced, and we selected GAL4-NR1I2 LBD clones that matched each consensus sequence.

Cell culture and luciferase reporter assays. COS7 cells were maintained in phenol-red–free Dulbecco's minimal Eagle medium (DMEM) supplemented with 10% fetal bovine serum (FBS). Twenty-four hours before transfection, we seeded 96-well plates with 5×10^5 cells per plate. Chimeric receptor plasmids were cotransfected along with the tk(MH100)x4luc and pCMX-β-galactosidase reporter plasmids using calcium-phosphate–mediated transfection (Grün et al. 2002; Tabb et al. 2004). All ligands were initially dissolved in dimethylsulfoxide (DMSO) and subsequently diluted in DMEM supplemented with 10% charcoal-resin stripped FBS with a final concentration of 0.5% DMSO. The final DMSO concentration was minimized according to the solubility limits of the test compounds and adjusted so that all treatments were carried out under the same conditions. No overt toxicity, as indicated by β-galactosidase activity, was observed relative to untreated controls. After 24 hr of ligand exposure, we assayed 50-μL aliquots of cell lysate for luciferase and β-galactosidase activity, as previously described (Grün et al. 2002). Luciferase activity is reported as fold activation relative to the vehicle control (0.5% DMSO) and normalized for β-galactosidase activity. Each combination of receptor and ligand was run in triplicate at three doses and repeated whenever the coefficient of variance exceeded 0.15. Positive control ligands were assigned based on previously published data or empirically determined upon cloning of the novel orthologs. We also ran a negative control consisting of vector lacking an NR1I2 LBD for each ligand to ensure luciferase activity was not promoted via LBD-independent pathways.

Sequence alignment and phylogenetic analysis. Novel sequences were checked for similarity using blastn and blastp (NCBI 2007a) and submitted to GenBank (NCBI 2007b). We used ClustalX (Thompson et al. 1997) to align deduced amino acid LBD sequences and create an identity matrix. A neighbor-joining phylogenetic tree was constructed using the PHYLIP computer program (Felsenstein 1989) using NR1I3 as a closely related outgroup.

Table 1. Compounds tested for their ability to activate NR1I2 orthologs.

Compound	Classification	CAS no.	Supplier
4-*tert*-Octylphenol	Alkyl phenol	140-66-9	Wako Pure Chemical Industries, Osaka, Japan
Carbaryl	Carbamate	63-25-2	ChemService, West Chester, PA, USA
Pentachlorophenol	Chlorinated phenol	87-86-5	Wako Pure Chemical Industries, Osaka, Japan
2,4-Dichlorophenol	Chlorinated phenol	120-83-2	Tokyo Chemical Industry, Japan
Benzophenone	Industrial intermediate	119-61-9	ChemService, West Chester, PA, USA
4-Nitrotoluene	Industrial intermediate	99-99-0	Tokyo Chemical Industry, Tokyo, Japan
Chlordane	Organochlorine	57-74-9	ChemService, West Chester, PA, USA
Dieldrin	Organochlorine	60-57-1	ChemService, West Chester, PA, USA
p,p′-DDE	Organochlorine	72-55-9	ChemService, West Chester, PA, USA
Methoxychlor	Organochlorine	72-43-5	ChemService, West Chester, PA, USA
o,p′-DDT	Organochlorine	789-02-6	ChemService, West Chester, PA, USA
Toxaphene	Organochlorine	8001-35-2	ChemService, West Chester, PA, USA
Endosulfan	Organochlorine	115-29-7	ChemService, West Chester, PA, USA
Octachlorostyrene	Organohalogen	29082-74-4	ChemService, West Chester, PA, USA
Tributyl tin chloride	Organotin	1461-22-9	Sigma-Aldrich, St. Louis, MO, USA
Triphenyl tin chloride	Organotin	639-58-7	Sigma-Aldrich, St. Louis, MO, USA
Dibutyl phthalate	Phthalate	84-74-2	Wako Pure Chemical Industries, Osaka, Japan
Benzyl butyl phthalate	Phthalate	85-68-7	Wako Pure Chemical Industries, Osaka, Japan
Bis (2-ethylhexyl) phthalate	Phthalate	117-81-7	Wako Pure Chemical Industries, Osaka, Japan
Dicyclohexyl phthalate	Phthalate	84-61-7	Wako Pure Chemical Industries, Osaka, Japan
Diethyl phthalate	Phthalate	84-66-2	Kanto Chemical Company, Tokyo, Japan
Di-*n*-hexyl phthalate	Phthalate	84-75-3	Tokyo Chemical Industry, Tokyo, Japan
n-Dipentyl phthalate	Phthalate	131-18-0	Tokyo Chemical Industry, Tokyo, Japan
n-Dipropyl phthalate	Phthalate	131-16-8	Tokyo Chemical Industry, Tokyo, Japan
Bisphenol A	Plastic monomer	80-05-7	Tokyo Chemical Industry, Tokyo, Japan
Fenvalerate	Pyrethroid	51630-58-1	ChemService, West Chester, PA, USA
Amitrol	Triazine	61-82-5	ChemService, West Chester, PA, USA

CAS, Chemical Abstracts Service; *p,p′*-DDE, *p,p′*-dichlorodiphenyldichloroethylene; *o,p′*-DDT, *o,p′* dichlorodiphenyltrichloroethane.

Results

NR1I2 ortholog sequences. Comparison of NR1I2 ortholog LBD sequences (Figure 1) revealed a relatively high degree of similarity among mammalian orthologs compared to nonmammals. Human SXR amino acid

residues that line the LBD and interact with various ligands (shaded) have been characterized by X-ray crystallography (Chrencik et al. 2005; Watkins et al. 2001, 2003). The corresponding residues appear to be highly conserved within mammals or are typically represented by functionally similar amino acid substitutions such as nonpolar valine, leucine, and methionine, or polar serine and threonine. Notable exceptions include the substitution of serine for leucine at position 105 in rodents and leucine or isoleucine for glutamine at position 184 in rabbits and rodents. When comparing nonmammalian NR1I2 orthologs, the least conserved region is the helix 1–3 insert, almost entirely absent in *Xenopus* BXRs, and highly variable among avian CXRs and fish orthologs. This region is thought to facilitate expansion of the ligand-binding pocket and distinguishes NR1I2 from functionally divergent members of the NR1I family (Moore et al. 2002).

Sequence similarity and associations observed in the neighbor-joining tree (Figure 2) are generally consistent with expected evolutionary relationships among the represented vertebrate classes and orders. These results also indicate that the nonmammalian orthologs are approximately equidistant from mammalian NR1I2 and NR1I3, consistent with the hypothesis that mammalian NR1I2 and NR1I3 resulted from a gene duplication of a nonmammalian ancestral ortholog (Handschin et al. 2004; Krasowski et al. 2005).

Activation of NR1I2 othologs. All ligands (with the exception of organotins) were screened at concentrations of 0.5, 5, and 50 μM. Of the 27 xenobiotic compounds tested, phthalates and organochlorines were most effective at activating NR1I2 orthologs. Human SXR and murine PXR were readily activated by most phthalates at 5 μM (Table 2), whereas amphibian, zebrafish, fugu, and medaka orthologs were for the most part unaffected, even at the highest concentrations. At 50 μM, all organochlorines except octachlorostyrene induced a > 10-fold increase in luciferase activity relative to vehicle alone in many species (Table 3). Nonprimate mammalian, avian, and amphibian NR1I2 orthologs appeared most susceptible to organochlorine activation and exhibited moderate (4- to 10-fold) to high luciferase activity at 5 μM. With the exception of 2,4-dichlorophenol in medaka, most NR1I2 orthologs were completely insensitive to chlorinated phenols. The organotins, which are cytotoxic at micromolar concentrations, were tested at 1, 10, and 100 nM and failed to induce significant luciferase activity in any species (Table 4). Among the nonorganochlorine pesticides and industrial compounds, only the pyrethroid ester fenvalerate and the alkyl phenol surfactant 4-*tert*-octylphenol elicited significant luciferase activity at the 5-μM concentration.

Figure 1. Alignment of amino acid sequences of NR1I2 ortholog LBDs. Shaded regions correspond to amino acid residues of the LBD that have been shown to interact with xenobiotic ligands in human SXR (Chrencik et al. 2005; Watkins et al. 2001, 2003). The boxed regions represent the helix 1–3 insert that distinguishes functionally divergent members of the NR1I subfamily (Moore et al. 2002). J. macaque, Japanese macaque; C.E. macaque, crab-eating macaque.

Discussion

Our results show significant variability across species in the capacity of xenobiotics to activate NR1I2 orthologs. Generally speaking, NR1I2 exhibits broad ligand specificity and regulates genes involved in hepatic metabolism of endogenous and xenobiotic compounds. As a result, this transcription factor presents unique challenges with regard to pharmacology and toxicology. For instance, the antibiotic rifampicin, a potent and selective activator of human SXR, can up-regulate hepatic metabolism of steroids to the extent that patients were incorrectly diagnosed with Cushing's syndrome following overnight dexamethasone suppression tests (Kyriazopoulou and Vagenakis 1992). Furthermore, activation of SXR by one therapeutic compound can significantly alter the fate of another. Rifampicin and the herbal supplement St. John's wort have both been shown to increase the clearance of the oral contraceptives ethinylestradiol and norethindrone (Barditch-Crovo et al. 1999; Hall et al. 2003).

Compounds that activated human SXR also activated SXR in nonhuman primates, but fold induction relative to the vehicle was typically lower in these species. In contrast, the nonprimate mammalian orthologs exhibited higher relative activation for many organochlorines and phthalates when compared to human SXR. Although fold induction of luciferase activity was variable across species for each ligand, all mammalian, avian, and amphibian orthologs appeared to be suitable qualitative models for predicting activation of human SXR with organochlorines. The two *Xenopus* BXRs had activation profiles similar to each other but were much less predictive of the human SXR response to phthalates compared to mammalian

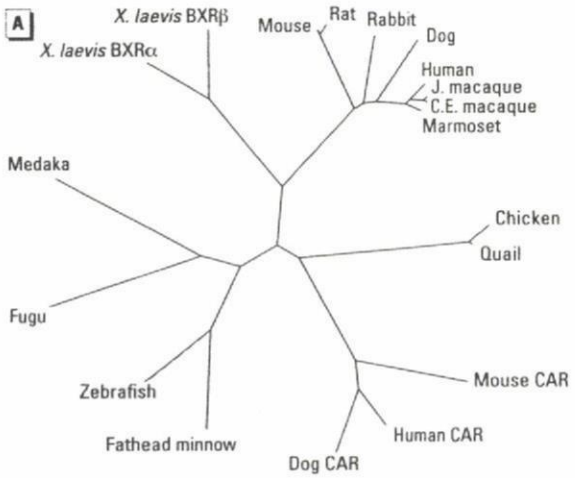

B

Human	J. macaque	C.E. macaque	Marmoset	Dog	Mouse	Rat	Rabbit	Chicken	Quail	X. laevis BXRα	X. laevis BXRβ	FHM	Zebrafish	Fugu	Medaka	
100	94	95	94	83	76	76	81	44	45	50	50	46	45	41	41	Human
	100	98	94	82	77	76	82	43	45	50	49	46	45	41	40	J. macaque
		100	94	83	77	76	82	44	45	50	49	47	45	41	40	C.E. macaque
			100	83	79	78	83	44	46	50	49	47	46	42	40	Marmoset
				100	75	75	78	43	45	48	48	47	44	42	39	Dog
					100	98	79	44	46	49	50	46	47	40	41	Mouse
						100	77	44	46	49	50	46	47	40	42	Rat
							100	44	45	49	50	45	44	39	39	Rabbit
								100	95	42	43	42	41	43	42	Chicken
									100	43	44	44	43	44	43	Quail
										100	81	45	46	47	46	*X. laevis* BXRα
											100	46	46	46	44	*X. laevis* BXRβ
												100	77	52	52	FHM
													100	51	49	Zebrafish
														100	59	Fugu
															100	Medaka

Figure 2. Nonrooted neighbor-joining tree of NR1I2 orthologs and mammalian NR1I3 ligand-binding domains (*A*), and the percent amino acid identities of NR1I2 otholog ligand-binding domains (*B*). Abbreviations: FHM, fathead minnow; J. macaque, Japanese macaque; C.E. macaque, crab-eating macaque.

Table 2. Species-specific activation of NR1I2 orthologs by phthalates.

Ligand	Exposure (μM)	Human	Japanese macaque	Crab-eating macaque	Marmoset	Dog	Mouse	Rat	Rabbit	Chicken	Quail	*X. laevis* BXRα	*X. laevis* BXRβ	FHM	Zebrafish	Fugu	Medaka
Diethyl phthalate	50	2.7	1.1	1.4	1.4	1.5	0.8	1.7	1.4	1.6	2.2	0.9	0.5	14.4	3.3	1.3	5.1
	5	1.0	0.6	0.7	0.8	1.0	0.5	0.9	0.7	0.9	1.0	0.7	1.0	2.4	0.7	1.1	3.3
	0.5	0.8	1.4	0.9	0.9	1.1	2.5	0.8	0.9	1.0	0.7	2.5	0.7	0.8	1.1	1.1	1.7
Benzyl butyl phthalate	50	11.4	4.8	3.6	4.4	12.0	23.6	18.9	12.0	7.1	10.1	3.1	2.0	8.5	1.8	1.6	1.4
	5	4.5	3.6	4.0	3.1	1.6	5.1	7.0	3.3	3.3	8.6	1.8	1.4	3.8	1.0	1.5	1.1
	0.5	1.0	1.4	1.3	1.0	1.4	1.1	1.1	0.9	1.2	1.7	1.0	0.7	1.0	0.7	0.8	1.0
Bis (2-ethylhexyl) phthalate	50	13.0	6.8	3.6	3.7	12.8	35.3	28.1	10.5	10.5	6.8	3.5	4.2	2.8	1.4	2.7	2.4
	5	10.7	12.4	9.8	5.8	3.5	33.6	30.0	6.7	6.3	6.3	1.9	3.8	1.7	1.1	3.7	2.3
	0.5	1.9	3.8	5.3	1.9	1.1	2.5	3.8	1.9	1.5	1.2	1.5	1.2	1.1	0.8	1.3	1.1
Dicyclohexyl phthalate	50	11.0	4.1	2.7	3.0	11.1	16.6	16.2	7.8	9.2	6.3	2.9	3.2	2.0	1.5	1.5	1.6
	5	10.1	5.5	5.8	5.7	3.7	12.1	10.4	3.0	5.8	7.9	1.9	2.9	1.6	2.7	2.5	1.3
	0.5	1.8	1.5	1.7	1.5	1.3	1.3	1.4	1.1	1.3	1.5	0.7	1.1	1.1	0.8	1.1	1.2
Dibutyl phthalate	50	10.9	4.2	4.5	4.2	9.9	19.6	19.5	10.5	7.9	5.4	2.3	1.0	14.1	2.7	1.6	1.9
	5	3.6	2.4	2.9	2.9	2.0	2.5	4.2	2.5	2.2	3.3	0.9	1.1	5.1	1.9	1.4	1.6
	0.5	2.5	1.4	1.1	1.0	1.0	0.7	1.1	1.1	1.1	0.9	1.1	1.1	0.9	0.8	1.0	1.0
n-Dipentyl phthalate	50	10.7	2.8	3.6	4.6	4.8	15.3	22.6	6.5	7.8	7.2	3.4	1.8	7.8	1.7	1.8	2.0
	5	2.6	2.9	4.0	4.1	0.6	4.2	5.9	2.2	2.9	7.5	3.4	1.4	1.6	0.8	2.4	1.5
	0.5	1.8	2.1	1.6	2.2	0.7	1.0	1.2	1.0	1.0	1.7	1.5	1.0	1.7	1.2	1.1	2.1
n-Dipropyl phthalate	50	8.1	4.0	4.6	6.3	2.0	8.8	12.3	4.4	6.8	5.7	5.0	1.0	36.2	6.2	2.3	5.7
	5	2.5	1.3	1.9	2.8	0.4	1.5	2.2	1.4	1.4	2.5	3.1	1.3	13.6	4.0	1.2	5.5
	0.5	2.2	0.7	1.0	1.4	0.4	1.0	1.1	0.7	0.9	1.1	1.1	0.8	2.4	0.6	1.3	2.3
Di-*n*-hexyl phthalate	50	10.6	3.7	3.7	5.1	3.4	20.1	21.4	4.9	9.5	10.5	4.3	2.5	6.4	1.6	2.4	1.5
	5	3.9	3.1	5.6	4.8	0.8	4.7	7.4	3.2	2.2	6.9	2.2	1.7	2.2	0.9	2.7	1.2
	0.5	1.2	1.0	1.8	1.9	0.5	0.9	1.1	0.7	1.0	1.5	2.0	1.1	1.1	0.7	1.5	1.4
Positive control[a]	50	22.8	5.9	7.3	14.6	17.8	68.6	41.3	10.2	17.7	22.8	32.1	94.0	—	—	5.8	12.8
	5	16.3	4.3	5.0	7.7	2.8	64.2	39.8	3.1	5.7	14.7	22.7	49.8	34.1	6.2	4.9	8.0
	0.5	3.7	1.6	2.2	2.6	1.4	36.7	26.6	1.0	1.0	4.4	10.9	8.8	24.2	3.0	2.4	2.6

FHM, fathead minnow. Values represent fold induction of luciferase activity (normalized for β-galactosidase activity) relative to DMSO treatment.
[a]Positive controls were as follows: rifampicin for human, macaque, dog, marmoset, rabbit, and fugu; pregnenolone 16α-carbonitrile for mouse and rat; 5β-3,20 pregnane dione for chicken and quail; *p*-hydroxy benzoic acid butyl ester for *Xenopus laevis BXRα and BXRβ*, and medaka; and clotrimazole (cytotoxic at 50 μM) for FHM and zebrafish.

and avian orthologs. In contrast, responses among fish orthologs were so variable that few if any generalizations could be made. Medaka appeared to be insensitive to the vast majority of compounds tested, whereas the fathead minnow appears to be the most relevant model with regard to human SXR activation.

An important aspect of interpreting the toxicologic relevancy of these data is the comparison of the concentrations that elicit *in vitro* activation to predicted environmental exposure. One major limitation to analysis is that there is a relative paucity of data concerning the concentrations of chemicals in blood and other biological fluids in response to particular

Table 3. Species-specific activation of NR1I2 orthologs by organochlorines and phenols.

Ligand	Exposure (μM)	Human	Japanese macaque	Crab-eating macaque	Marmoset	Dog	Mouse	Rat	Rabbit	Chicken	Quail	*X. laevis* BXRα	*X. laevis* BXRβ	FHM	Zebrafish	Fugu	Medaka
Chlordane	50	5.7	3.1	4.4	7.8	21.3	20.7	12.0	12.1	9.5	7.5	17.9	7.2	14.4	4.5	2.7	0.5
	5	8.9	3.7	3.3	5.8	5.1	10.8	14.4	6.7	5.3	10.6	4.3	5.1	7.9	2.4	3.0	0.8
	0.5	2.3	1.1	1.4	2.6	1.4	2.2	2.7	2.6	1.5	4.0	1.2	1.6	1.8	0.9	1.1	0.7
o,p'-DDT	50	16.3	5.1	6.9	12.3	27.0	45.3	32.3	12.6	17.3	23.8	16.7	15.8	11.9	4.0	9.1	1.3
	5	6.2	1.6	2.1	4.1	1.0	3.0	3.4	1.6	3.6	7.4	2.0	2.6	2.4	1.3	1.6	1.1
	0.5	1.3	1.1	1.1	1.0	0.8	1.1	0.6	0.9	1.2	1.3	1.1	1.2	1.1	1.0	1.3	1.2
p,p'-DDE	50	15.4	2.8	8.5	12.0	5.3	8.6	9.6	3.8	12.6	7.4	5.4	8.6	1.8	1.1	4.3	1.1
	5	2.1	1.2	1.4	2.2	0.7	1.2	1.1	1.0	1.7	1.6	1.4	1.7	1.4	0.6	1.1	1.1
	0.5	1.2	0.8	0.8	1.2	0.9	1.3	0.7	0.9	1.1	1.0	0.9	1.3	1.0	0.9	0.9	1.1
Dieldrin	50	11.0	3.4	5.9	11.6	9.8	33.0	25.7	16.3	10.4	13.8	9.3	4.8	5.6	1.6	2.8	0.2
	5	7.0	1.3	3.8	5.7	2.8	8.2	7.4	11.6	2.7	9.0	2.5	3.6	2.1	1.0	1.7	0.3
	0.5	2.0	1.1	1.3	3.3	1.0	1.5	1.6	2.2	1.4	3.4	1.3	1.8	2.2	1.0	1.0	0.5
Endosulfan	50	8.5	4.6	4.7	14.6	17.5	50.7	29.9	16.8	17.8	15.4	18.0	9.9	7.1	3.5	2.8	0.3
	5	4.7	2.6	3.1	5.6	1.3	7.0	9.1	8.6	3.3	7.8	1.9	3.0	2.5	1.0	1.4	0.3
	0.5	1.5	1.2	1.5	2.3	2.4	1.7	1.5	1.7	1.1	2.4	1.1	1.3	1.8	1.0	1.1	0.8
Methoxychlor	50	22.3	4.1	10.6	21.8	12.5	110.0	57.9	16.1	24.8	20.8	11.2	9.4	7.1	3.4	7.1	0.6
	5	3.9	1.5	2.4	3.9	1.0	16.5	29.8	2.5	3.5	5.2	1.7	2.5	2.0	1.4	1.3	1.0
	0.5	1.2	1.2	0.7	1.5	0.8	1.3	1.0	0.9	1.2	2.0	1.1	1.4	1.4	1.2	0.9	1.4
Octachlorostyrene	50	8.5	3.1	2.4	2.9	3.5	5.2	6.6	2.1	3.7	3.9	2.7	1.0	1.2	0.9	1.3	1.3
	5	1.3	1.0	1.1	1.2	1.4	1.2	1.4	0.9	1.1	2.3	0.7	0.7	1.9	0.6	1.3	1.2
	0.5	1.4	0.9	0.8	0.9	0.8	0.6	0.9	0.9	1.0	1.4	0.6	0.6	1.7	1.1	1.0	1.4
Toxaphene	50	10.9	5.1	6.5	16.3	41.9	38.2	22.4	16.3	16.0	25.8	21.5	12.5	19.8	5.5	2.8	0.8
	5	8.5	4.1	4.8	10.7	7.5	17.2	17.8	6.3	8.0	14.0	5.1	8.3	14.9	3.1	3.3	0.8
	0.5	1.9	1.1	1.3	2.6	0.7	2.3	1.9	0.9	1.7	4.7	1.3	1.8	3.7	1.2	1.1	1.0
2,4-Dichlorophenol	50	1.0	0.6	0.9	1.3	0.4	1.3	0.9	0.9	1.1	0.8	2.5	0.7	0.9	0.6	0.8	2.7
	5	1.1	0.8	1.1	1.4	0.3	1.2	0.9	0.7	1.0	1.0	1.4	0.8	1.8	0.7	1.0	5.0
	0.5	0.9	0.8	1.2	1.4	0.5	0.7	1.0	0.7	1.1	1.3	0.9	0.9	1.7	1.0	1.1	5.7
Pentachlorophenol	50	0.8	0.9	1.4	1.3	0.3	1.5	1.0	0.7	0.7	0.9	1.3	1.4	0.8	0.5	1.0	1.3
	5	1.7	0.9	1.5	1.2	0.4	3.1	1.0	0.6	0.8	1.0	2.3	1.1	1.0	0.8	1.2	1.1
	0.5	0.8	0.8	1.0	1.1	0.4	0.6	1.0	0.7	1.1	0.9	2.8	0.9	0.7	0.7	1.1	1.2

FHM, fathead minnow. Values represent fold induction of luciferase activity (normalized for β-galactosidase activity) relative to DMSO treatment.

Table 4. Species-specific activation of NR1I2 orthologs by selected nonorganochlorine pesticides, organotins, and industrial compounds.

Ligand	Exposure (μM)	Human	Japanese macaque	Crab-eating macaque	Marmoset	Dog	Mouse	Rat	Rabbit	Chicken	Quail	*X. laevis* BXRα	*X. laevis* BXRβ	FHM	Zebrafish	Fugu	Medaka
4-Nitrotoluene	50	2.1	0.6	1.1	1.5	0.4	1.6	1.2	0.9	1.3	1.1	2.3	0.9	1.0	0.9	1.4	6.6
	5	1.0	0.8	1.0	1.4	0.4	1.1	1.3	1.1	1.0	0.9	2.1	1.1	1.3	0.7	1.4	5.1
	0.5	0.8	1.2	1.0	1.7	0.7	0.8	1.0	2.0	1.6	1.0	1.1	1.1	1.3	0.7	1.8	2.0
4-*tert*-Octylphenol	50	15.9	3.5	4.0	7.3	12.8	13.4	20.4	7.5	8.7	7.7	12.5	5.2	17.1	4.6	3.3	6.0
	5	10.2	2.0	3.2	4.4	2.4	1.7	2.3	1.4	5.4	6.5	4.8	2.3	6.0	3.1	3.6	6.4
	0.5	1.3	1.0	1.5	1.6	0.5	0.7	1.0	1.0	1.4	2.6	1.1	1.2	1.4	0.9	1.5	6.7
Amitrol	50	0.7	1.0	0.8	1.1	0.3	2.2	1.0	0.5	1.0	1.3	1.7	0.8	0.9	0.7	1.1	4.2
	5	2.0	0.7	1.1	1.7	0.5	0.6	0.9	0.7	1.0	1.4	1.4	0.7	1.1	0.9	1.7	6.5
	0.5	4.3	2.3	1.6	2.2	0.9	1.3	1.3	2.6	1.5	4.6	3.0	1.2	3.5	1.0	1.5	6.3
Bisphenol A	50	11.0	3.8	3.7	5.4	1.0	3.0	2.5	4.8	9.2	6.3	6.0	5.3	2.8	2.3	4.9	3.5
	5	1.9	0.7	0.8	1.5	0.3	0.8	1.8	1.3	1.6	1.5	1.3	1.2	0.8	0.8	1.1	3.2
	0.5	0.9	0.7	0.8	1.1	0.4	0.9	1.0	0.7	1.1	1.2	1.2	0.8	0.8	0.8	1.6	2.1
Benzophenone	50	1.1	1.4	1.2	1.3	0.9	0.8	1.2	0.8	2.1	2.5	20.0	0.5	1.6	0.7	0.8	1.8
	5	0.9	1.1	0.8	0.9	1.9	0.9	0.8	0.7	1.1	1.3	7.9	0.7	1.1	0.8	1.0	1.5
	0.5	1.5	1.3	0.9	0.9	1.1	1.0	1.3	2.0	1.1	2.1	1.3	0.7	1.1	0.5	0.9	1.2
Carbaryl	50	2.3	0.9	1.9	3.0	1.8	1.8	1.2	2.3	1.5	2.1	1.7	1.6	2.0	1.4	1.2	1.7
	5	1.5	0.8	1.1	1.5	0.9	1.4	0.9	1.4	1.5	2.3	1.1	2.0	1.4	1.4	0.9	0.8
	0.5	2.8	1.5	2.1	2.6	1.2	2.3	2.0	1.9	1.9	3.9	1.6	2.3	2.7	1.3	1.4	0.8
Fenvalerate	50	13.7	6.6	10.4	19.8	60.7	65.9	41.7	32.8	23.5	23.3	11.6	11.8	4.0	6.2	8.4	1.0
	5	12.6	4.1	6.6	8.4	5.2	29.2	28.6	7.8	11.6	9.7	5.2	6.1	3.4	3.1	4.1	1.0
	0.5	2.0	0.9	1.8	2.0	1.0	1.6	1.9	1.6	1.6	1.6	1.2	1.3	1.4	0.9	1.0	1.0
Tributyl tin chloride	100	2.0	0.8	0.9	0.7	1.3	1.4	0.6	1.4	1.3	0.9	0.7	1.8	0.6	0.7	0.5	0.9
	10	0.9	1.0	0.8	0.7	1.2	1.0	0.6	0.7	1.3	1.3	0.8	1.2	0.6	0.7	0.8	0.9
	1	0.9	0.8	0.8	0.8	0.8	0.7	1.0	1.2	1.1	0.8	0.7	0.9	0.9	0.4	1.0	1.1
Triphenyl tin chloride	100	0.5	1.0	0.8	1.3	1.1	0.6	0.7	2.7	1.4	0.9	0.9	1.0	0.8	2.0	1.7	0.9
	10	1.1	0.7	0.9	0.9	1.6	0.3	1.4	1.0	0.9	0.8	0.6	1.2	1.3	0.9	1.9	1.1
	1	0.7	1.0	1.0	0.8	1.2	0.4	0.8	2.1	0.9	1.0	0.6	1.1	0.9	0.8	1.2	1.2

FHM, fathead minnow. Values represent fold induction of luciferase activity (normalized for β-galactosidase activity) relative to DMSO treatment.

environmental concentrations. Another limitation to meaningful comparisons is that the method of reporting concentrations in biological and environmental samples is quite variable. For instance, the concentrations of many of the same organochlorine pesticides and phthalates used in this study have been measured in human breast milk as an indicator of neonatal exposure. The concentrations of organochlorines and other lipophilic compounds are reported as nanograms per gram lipid, and the major metabolites of phthalates, phthalate monoesters, are reported micrograms per liter. Assuming an average of 3–4% lipid in breast milk (Needham and Wang 2002), molar concentrations of organochlorines such as methoxychlor and *o,p′*-DDT were typically < 1 nM, whereas endosulfan and *p,p′*-DDE were in the 10–50 nM range (Damgaard et al. 2006; Shen et al. 2008). Although concentrations in breast milk are an order of magnitude lower than the minimum dose tested (500 nM), the daily intake of the infant should also be considered. Nanomolar to low micromolar concentrations were reported for phthalate monoesters in the breast milk of Danish and Finnish women (Main et al. 2006). Based on the concentrations in breast milk, infant body mass, and average milk consumption, the range of the estimated daily intake of some phthalates exceeded 50 μg/kg/day, the same dose used to up-regulate PXR-responsive genes with known ligands in laboratory mice (Xie et al. 2000a).

Although the toxicologic effects of activating NR1I2 are not completely understood, the metabolic pathways regulated by NR1I2 implicate it as a potential target for disrupting bile acid and steroid homeostasis (Zhai et al. 2007). Further complicating these interactions, xenobiotics that fail to activate this receptor may be more toxic than those that activate it and induce their own metabolism. NR1I2 mediates the metabolism of many drugs, and this metabolism can be induced to a very high level by chronic NR1I2 activation. Mice expressing a constitutively active form of human SXR (Alb-VPSXR) are almost completely resistant to the anesthetic effects of tribromoethanol and zoxaolamine, demonstrating this concept (Xie et al. 2000a).

The development of competitive binding and receptor activation assays allows one to estimate the potential for a xenobiotic compound to interact with a single receptor in any species. However, the ability to predict which chemicals will induce a characterized response *in vivo* at a particular dose, such as uterine proliferation via estrogen receptor (ER) activation, is much more complex. This matter is further complicated when considering exposure to a chemical that activates multiple transcription factors with different affinities. For instance, bisphenol A has an EC_{50} (half maximal concentration) of approximately 200 nM in ER luciferase reporter assays and the E-Screen cell proliferation assay (Gutendorf and Westendorf 2001). Our data indicate that bisphenol A activates NR1I2-dependent transcription at 50 μM and thus would induce its own metabolism at similar concentrations. Based on these data, one might predict an inverted U-shaped dose–response curve for bisphenol A *in vivo*, a phenomenon that has been repeatedly reported (for review, see vom Saal and Hughes 2005).

A significant difficulty in deriving an accurate risk assessment from laboratory experiments is the uncertainty about whether the underlying mechanisms of response to chemical exposure are universal. The use of *in vitro* or cell-based assays to guide and refine the development of *in vivo* models to screen compounds for NR1I2 activation is a useful tool to understand and/or prevent unintended xenobiotic interactions. Our results demonstrate species-specific differences in the ability of NR1I2 orthologs to activate transcription. This suggests that the metabolism, and presumably the physiological effects, of those ligands will also vary across species. Future work screening xenobiotics for toxicologic effects as well as drug–drug interactions should take these data into consideration.

References

Barditch-Crovo P, Trapnell CB, Ette E, Zacur HA, Coresh J, Rocco LE, et al. 1999. The effects of rifampin and rifabutin on the pharmacokinetics and pharmacodynamics of a combination oral contraceptive. Clin Pharmacol Ther 65(4):428–438.

Blumberg B, Sabbagh W Jr, Juguilon H, Bolado J Jr, van Meter CM, Ong ES, et al. 1998. SXR, a novel steroid and xenobiotic-sensing nuclear receptor. Genes Dev 12(20):3195–3205.

Chrencik JE, Orans J, Moore LB, Xue Y, Peng L, Collins JL, et al. 2005. Structural disorder in the complex of human pregnane X receptor and the macrolide antibiotic rifampicin. Mol Endocrinol 19(5):1125–1134.

Damgaard IN, Skakkebæk NE, Toppari J, Virtanen HE, Shen H, Schramm KW, et al. 2006. Persistent pesticides in human breast milk and cryptorchidism. Environ Health Perspect 114:1133–1138.

Dussault I, Forman BM. 2002. The nuclear receptor PXR: a master regulator of "homeland" defense. Crit Rev in Eukar Gene 12(1):53–64.

Einarsson K, Gustafsson JA. 1973. Effects of a potent catatoxic steroid, 16 -cyanopregnenolone, on microsomal metabolism of steroid hormones, sterols and bile acids in rats. Eur J Biochem 32(2):197–206.

Felsenstein J. 1989. PHYLIP - Phylogeny Inference Package (Version 3.2). Cladistics 5:164–166.

Grün F, Venkatesan RN, Tabb MM, Zhou C, Cao J, Hemmati D, et al. 2002. Benzoate X receptors alpha and beta are pharmacologically distinct and do not function as xenobiotic receptors. J Biol Chem 277(46):43691–43697.

Gutendorf B, Westendorf J. 2001. Comparison of an array of in vitro assays for the assessment of the estrogenic potential of natural and synthetic estrogens, phytoestrogens and xenoestrogens. Toxicology 166(1-2):79–89.

Hall SD, Wang Z, Huang SM, Hamman MA, Vasavada N, Adigun AQ, et al. 2003. The interaction between St John's wort and an oral contraceptive. Clin Pharmacol Ther 74(6):525–535.

Handschin C, Blattler S, Roth A, Looser R, Oscarson M, Kaufmann MR, et al. 2004. The evolution of drug-activated nuclear receptors: one ancestral gene diverged into two xenosensor genes in mammals. Nucl Recept 2:7; doi:10.1186/1478-1336-2-7 [Online 12 October 2004].

Jones SA, Moore LB, Shenk JL, Wisely GB, Hamilton GA, McKee DD, et al. 2000. The pregnane X receptor: a promiscuous xenobiotic receptor that has diverged during evolution. Mol Endocrinol 14(1):27–39.

Kliewer SA, Goodwin B, Willson TM. 2002. The nuclear pregnane X receptor: a key regulator of xenobiotic metabolism. Endocr Rev 23(5):687–702.

Kliewer SA, Moore JT, Wade L, Staudinger JL, Watson MA, Jones SA, et al. 1998. An orphan nuclear receptor activated by pregnanes defines a novel steroid signaling pathway. Cell 92(1):73–82.

Krasowski MD, Yasuda K, Hagey LR, Schuetz EG. 2005. Evolutionary selection across the nuclear hormone receptor superfamily with a focus on the NR1I subfamily (vitamin D, pregnane X, and constitutive androstane receptors). Nucl Recept 3:2; doi:10.1186/1478-1336-3-2 [30 September 2005].

Kretschmer XC, Baldwin WS. 2005. CAR and PXR: xenosensors of endocrine disrupters? Chem Biol Interact 155(3):111–128.

Kyriazopoulou V, Vagenakis AG. 1992. Abnormal overnight dexamethasone suppression test in subjects receiving rifampicin therapy. J Clin Endocrinol Metab 75(1):315–317.

Lehmann JM, McKee DD, Watson MA, Willson TM, Moore JT, Kliewer SA. 1998. The human orphan nuclear receptor PXR is activated by compounds that regulate CYP3A4 gene expression and cause drug interactions. J Clin Invest 102(5):1016–1023.

Li C, Evans RM. 1997. Ligation independent cloning irrespective of restriction site compatibility. Nucleic Acids Res 25(20):4165–4166.

Main KM, Mortensen GK, Kaleva MM, Boisen KA, Damgaard IN, Chellakooty M, et al. 2006. Human breast milk contamination with phthalates and alterations of endogenous reproductive hormones in infants three months of age. Environ Health Perspect 114:270–276.

Moore LB, Maglich JM, McKee DD, Wisely B, Willson TM, Kliewer SA, et al. 2002. Pregnane X receptor (PXR), constitutive androstane receptor (CAR), and benzoate X receptor (BXR) define three pharmacologically distinct classes of nuclear receptors. Mol Endocrinol 16(5):977–986.

National Center for Biotechnology Information. 2007a. BLAST Home. Available: http://www.ncbi.nlm.nih.gov/BLAST/ [accessed 29 May 2008].

National Center for Biotechnology Information. 2007b. GenBank Overview. Available: http://www.ncbi.nlm.nih.gov/Genbank/index.html [accessed 29 May 2008].

Needham LL, Wang RY. 2002. Analytic considerations for measuring environmental chemicals in breast milk. Environ Health Perspect 110:A317–A324.

Selye H. 1971. Hormones and resistance. J Pharm Sci 60(1):1–28.

Shen H, Main KM, Andersson AM, Damgaard IN, Virtanen HE, Skakkebæk NE, et al. 2008. Concentrations of persistent organochlorine compounds in human milk and placenta are higher in Denmark than in Finland. Human Reprod 23(1):201–210.

Tabb MM, Kholodovych V, Grün F, Zhou C, Welsh WJ, Blumberg B. 2004. Highly chlorinated PCBs inhibit the human xenobiotic response mediated by the steroid and xenobiotic receptor (SXR). Environ Health Perspect 112:163–169.

Thompson JD, Gibson TJ, Plewniak F, Jeanmougin F, Higgins DG. 1997. The CLUSTAL_X windows interface: flexible strategies for multiple sequence alignment aided by quality analysis tools. Nucleic Acids Res 25(24):4876–4882.

vom Saal FS, Hughes C. 2005. An extensive new literature concerning low-dose effects of bisphenol A shows the need for a new risk assessment. Environ Health Perspect 113:926–933.

Watkins RE, Maglich JM, Moore LB, Wisely GB, Noble SM, Davis-Searles PR, et al. 2003. 2.1 A crystal structure of human PXR in complex with the St. John's wort compound hyperforin. Biochemistry 42(6):1430–1438.

Watkins RE, Wisely GB, Moore LB, Collins JL, Lambert MH, Williams SP, et al. 2001. The human nuclear xenobiotic receptor PXR: structural determinants of directed promiscuity. Science 292(5525):2329–2333.

Xie W, Barwick JL, Downes M, Blumberg B, Simon CM, Nelson MC, et al. 2000a. Humanized xenobiotic response in mice expressing nuclear receptor SXR. Nature 406(6794):435–439.

Xie W, Barwick JL, Simon CM, Pierce AM, Safe S, Blumberg B, et al. 2000b. Reciprocal activation of xenobiotic response genes by nuclear receptors SXR/PXR and CAR. Genes Dev 14(23):3014–3023.

Xie W, Uppal H, Saini SP, Mu Y, Little JM, Radominska-Pandya A, et al. 2004. Orphan nuclear receptor-mediated xenobiotic regulation in drug metabolism. Drug Discov Today 9(10):442–449.

Zhai Y, Pai HV, Zhou J, Amico JA, Vollmer RR, Xie W. 2007. Activation of pregnane X receptor disrupts glucocorticoid and mineralocorticoid homeostasis. Mol Endocrinol 21(1):138–147.